7. SITE 753[1]

Shipboard Scientific Party[2]

HOLE 753A

Date occupied: 12 May 1988

Date departed: 13 May 1988

Time on hole: 13 hr, 45 min

Position: 30°50.340′S, 93°35.394′E

Bottom felt (rig floor; m; drill-pipe measurement): 1187.0

Distance between rig floor and sea level (m): 10.87

Water depth (drill-pipe measurement; corrected m): 1176.1

Total depth (rig floor; corrected m): 1249.8

Penetration (m): 62.8

Number of cores: 7

Total length of cored section (m): 62.8

Total core recovered (m): 61.06

Core recovery (%): 97

Oldest sediment cored:
Depth sub-bottom (m): 62.8
Nature: calcareous chalk
Earliest age: middle Eocene
Measured velocity (km/s): approximately 1.6

HOLE 753B

Date occupied: 13 May 1988

Date departed: 13 May 1988

Time on hole: 11 hr, 15 min

Position: 30°50.310′S, 93°35.394′E

Bottom felt (rig floor; m; drill-pipe measurement): 1187.0

Distance between rig floor and sea level (m): 10.87

Water depth (drill-pipe measurement; corrected m): 1176.1

Total depth (rig floor; corrected m): 1287.2

Penetration (m): 100.2

Number of cores: 7

Total length of cored section (m): 48.2

Total core recovered (m): 0.04

Core recovery (%): 0

Oldest sediment cored:
Depth sub-bottom (m): 90.50
Nature: calcareous chalk
Earliest age: middle Eocene

Principal results: Ocean Drilling Program (ODP) Site 753 is near the northern margin of the crest of Broken Ridge, about 28 km north of the main southward-dipping escarpment. The site was positioned to penetrate the youngest of the sediments that are unambiguously truncated by the prominent unconformity developed on Broken Ridge. Coring at Site 753, along with that at Site 752 and proposed Sites BR-3 and BR-4, was designed to provide a continuous section through the northward-dipping sediments below the truncation surface. The thickness of the subhorizontal pelagic sediments above the unconformity is less than 50 m at Site 753.

The site position was selected at shotpoint 820 of line 20 of the seismic survey conducted during Cruise 2708 of *Robert D. Conrad* (RC2708). Individual seismic reflectors can be correlated with confidence between the RC2708 survey and that made by *JOIDES Resolution* prior to drilling on Broken Ridge. The truncation surface can be identified at 0.052 s two-way traveltime (TWT) below seafloor (bsf) on the 3.5-kHz echo-sounder, and traces of northward-dipping reflectors are discernable below the unconformity.

Hole 753A was cored with the advanced hydraulic piston corer (APC) to 63 m below seafloor (mbsf), at which point the piston core barrel became stuck and could not be retrieved. Hole 753B, which is about 50 m north of Hole 753A, was washed down to 62 mbsf and cored with the extended core barrel (XCB) to 100 mbsf without significant recovery. We attribute the absence of cores from Hole 753B to the failure of the hinge pin holding the flapper of the float valve, which resulted in blockage of the core barrel.

Two lithologic units are recognized at Site 753:

Unit I (0–43.6 mbsf): Pliocene to lower Miocene foraminifer/nannofossil ooze. The sediment color changes from very pale brown to light gray in the top 2 m, grading to white at 34 mbsf, to alternating pale brown and white layers of similar thickness in the bottom 10 m of the unit. Mottling is sporadic and faint above, and common and distinct below, 24.4 mbsf. The nannofossil ooze in the bottom 10 m of Unit I is notably stiffer than that above and contains two closely spaced layers of limestone pebbles with 10% quartz. Trace amounts of volcanic glass, opaques, quartz, and radiolarians are present throughout. Individual grains are sand to silt size.

Unit II (43.6–62.8 mbsf): middle Eocene calcareous and foraminifer-bearing nannofossil chalk. In general, the sediment color in the upper part of the unit is white, with light greenish gray, millimeter-scale planar laminae that become more distinct with depth. In the lower part of Unit II, sediment color is also white, grading into pale yellow where ash layers are present. Sediment texture is similar to that of the overlying unit, but a 5% clay-size fraction at the top of Unit II increases to 11% at the bottom. Trace amounts of quartz, opaques, and volcanic glass (in the lower chalks) occur throughout.

The truncation surface, observed in the seismic-reflection and 3.5-kHz echo-sounder data, is at the top of Unit II. It represents a depositional hiatus between nannofossil Zones CP13c and CN1,2 (43–47 and 17–23.5 Ma, respectively). Other hiatuses are suspected in the Neogene Unit I because nannofossil Zone CN3 is missing at 34 mbsf and Zones CN5–7 are missing at 24 mbsf.

Planktonic/benthic foraminifer ratios suggest that Unit I was deposited in water depths of 600–2000 m (middle to lower bathyal) whereas middle Eocene Unit II was deposited in depths of 1000–1500 m (lower bathyal). However, the presence of limestone pebbles just above the truncation surface in Unit I suggests clastic deposition in shallow water.

Paleomagnetic measurements on Site 753 cores suggest that a zone of normal polarity occurs below the unconformity, from the top of Unit II to 47 mbsf. Reversed polarity characterizes the underlying interval down to the base of the recovered section. The normal and reversed intervals are tentatively correlated using the observed biostratigraphy as Chrons 20 and 20R.

---

[1] Peirce, J., Weissel, J., et al., 1989. *Proc. ODP, Init. Repts.*, 121: College Station, TX (Ocean Drilling Program).

[2] Shipboard Scientific Party is as given in the list of Participants preceding the contents.

On the basis of downhole temperature measurements in Holes 752A and 753A and thermal-conductivity measurements on sediments recovered from the two holes, the heat flow at Broken Ridge is 43.4 mW/m^2 (1.01 HFU). This value lies between the two measurements reported previously for Broken Ridge and is consistent with a thermal age of about 115 Ma derived from the empirically determined curve for global heat flow vs. age.

The principal result from Site 753, in light of the drilling at Hole 752A, is that Broken Ridge was uplifted by at least 1 km between the deposition of middle Eocene Unit II at Site 753, which lies below the truncation surface, and upper Eocene shallow-water sediments overlying the unconformity at Hole 752A. The age difference between these units is small (< ~5 m.y.), reflecting rapid tectonic uplift during a middle Eocene rifting event and fast erosion of the crest of Broken Ridge.

BACKGROUND AND OBJECTIVES

Overview

A detailed discussion of the background and objectives for drilling at Broken Ridge during ODP Leg 121 is found in the "Leg 121 Background and Objectives" chapter and the "Background and Objectives" section of the "Site 752" chapter (this volume). The particular drilling objectives for Site 753 are described in this section.

Drilling Objectives for Site 753

Site 753 (proposed Site BR-1) is at the northern end of a north-south transect of drill sites along the crest of Broken Ridge (Fig. 1). The transect was designed to sample the entire dipping, truncated sequence at Broken Ridge with single-bit holes, positioned to ensure some overlap of section between sites. Unfortunately, because of mechanical problems with coring, Site 753 was terminated after penetrating 100 m in Holes 753A and 753B. Thus, Site 753 does not overlap stratigraphically with Site 752 (proposed Site BR-2) to the south, and about 190 m of section remains unsampled in the upper part of the dipping and truncated sequence at Broken Ridge.

The principal drilling objective at Site 753 was to recover the stratigraphically highest sediments in the dipping and truncated sedimentary sequence at Broken Ridge (Fig. 2). Less than 50 m of pelagic ooze overlies the angular unconformity at Site 753.

The age, lithology, and depth of deposition of the youngest sediments clearly truncated by the erosional unconformity at Broken Ridge are information critical to a better understanding of the response of the lithosphere to the rifting process. If open-ocean pelagic sediments deposited in water depths of approximately 1000 m are found at Site 753, these would be interpreted as pre-rift sediments, and the duration of rifting would be less than the difference in the age of the uppermost of the truncated strata and magnetic anomaly 18 (~42 Ma), which lies to the south of Broken Ridge. A short duration of rifting would favor flexural uplift of Broken Ridge during rifting, which is a mechanical rather than a thermal consequence of lithospheric extension. If, on the other hand, the sediments below the unconformity are shallow-water clastics, rifting between Broken Ridge and Kerguelen Plateau began earlier (Maestrichtian?) than the age of those sediments, and the duration of rifting would therefore be much longer. For this latter case, the development of the erosional unconformity at Broken Ridge would include a second erosional event possibly related to a sea-level drop of sufficient magnitude to expose the crest of Broken Ridge a second time.

Although drilling at Site 753 was terminated prematurely due to mechanical problems with coring, the principal drilling objective was met by the recovery of middle Eocene lower bathyal chalks in two cores (121-753A-6H and 121-753A-7H) beneath the truncation surface.

OPERATIONS

Site 753

After considering the options resulting from the close spacing of the shallow-water prospective sites, we decided to meet the time and science objectives by moving the ship to prospective Site BR-1 before pursuing deeper drilling at Site 752 with the rotary coring system. The outcome of operations at prospective Sites BR-1 and BR-3 then would be used in deciding whether to return to Site 752.

JOIDES Resolution made the 2-nmi transit from Site 752 to prospective Site BR-1 in dynamic-positioning (DP) mode with the hydrophones up. The end of the transit occurred during a Global Positioning System (GPS) window, which allowed an accurate beacon drop at 1630 hr (local time), 12 May, while holding position over the site. During the short transit the stuck XCB barrel was removed from the bottom-hole assembly, and the pipe was ready to be run when the vessel went to full DP mode over the new beacon.

Hole 753A

Hole 735A was spudded at 2020 hr, with the mud line established by an APC core at 1187.0 m below the rig floor. We successfully took seven piston cores and two water samples with heatflow measurements (after Cores 121-753A-3H and 121-753A-6H). Core 121-753A-8H passed through the unconformity into stiffer material slightly deeper than at Hole 752A and became stuck. This time the core barrel parted with an overpull in excess of 160,000 lb as the ship heaved upward while attempting to pull the core barrel loose. Total penetration in Hole 753A was 62.8 mbsf, with 97% recovery (Table 1). The junk terminated Hole 753A, and the bit was pulled clear of the seafloor at 0615 hr, 13 May.

Hole 753B

JOIDES Resolution was offset 50 m north, and the pipe was washed to a depth of 24.4 mbsf to take a spot core. The core barrel of the XCB system came up empty for Core 121-753B-2X and was dropped to serve as a wash barrel while the pipe was drilled down to 61.6 mbsf. We planned to resume XCB coring at a depth that would slightly overlap the termination of piston coring in Hole 753A. This second wash core recovered only two or three small lumps of gritty chalk. Four XCB cores were attempted from that point to a depth of 100.2 mbsf; only nominal traces of chalk and fine sand were recovered (Table 1). We decided that either the formation could not be cored by XCB techniques or something unknown was wrong with the coring system. Drilling at the site was terminated, and the pipe was pulled, with the bit arriving on deck at 1725 hr, 13 May.

On deck, we determined the cause of our problem with core recovery. The hinge pin of the standard float-valve flapper was sheared, and the flapper was bridged across the throat of the bit. This prevented the XCB core barrel from extending beyond the bit, in addition to inhibiting any core material from reaching the core barrel. Impact marks on the damaged flapper suggested that it had been struck many times and that the first XCB barrel dropped had probably broken the hinge pin.

LITHOSTRATIGRAPHY AND SEDIMENTOLOGY

Sediments of Pliocene through middle Eocene age were recovered at Site 753 before drilling was terminated in Lutetian chalks. Two lithologic units are recognized at Site 753: Unit I, a 43.6-m-thick Pliocene to lower Miocene foraminifer and nannofossil ooze, and Unit II, a 19.2-m-thick middle Eocene chalk sequence (Table 2 and Fig. 3).

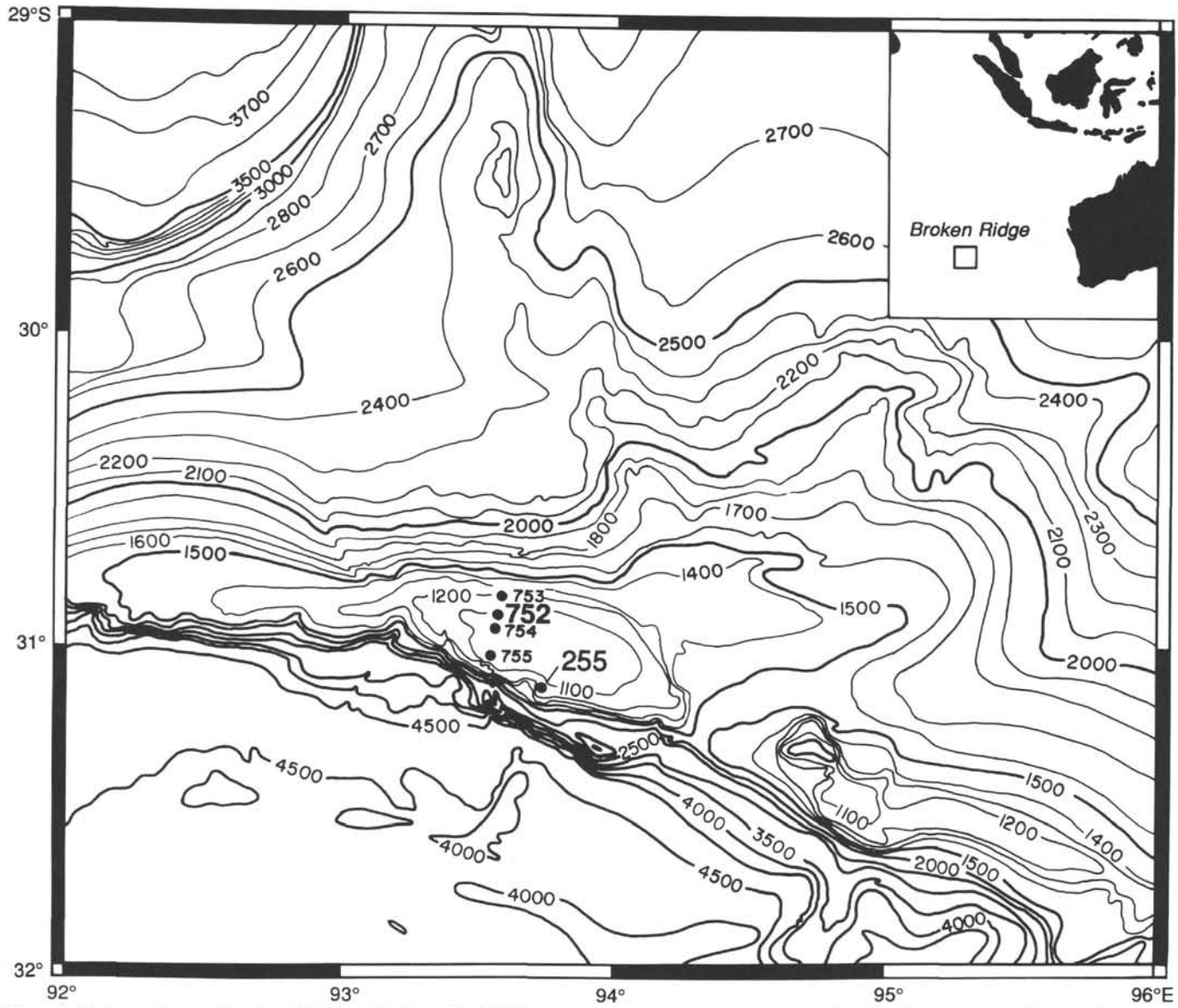

Figure 1. Bathymetric map showing ODP Site 753, Deep Sea Drilling Project (DSDP) Site 255, and other Leg 121 sites at Broken Ridge. Bathymetry, which is based mainly on RC2708 echo-sounder data, is contoured at 100-m intervals except along the south-facing escarpment, where contours are omitted for clarity.

Unit I (0–43.6 mbsf) is a foraminifer/nannofossil ooze that ranges in color from very pale brown (10YR 7/3) to light gray (10YR 7/3) in the top 2 m and grades down to white (10YR 8/1 or 10YR 8/2) at 34.0 mbsf. The sediment between 0 and 24.4 mbsf is predominantly homogeneous with sporadic faint mottling; mottling is both common and distinct for the remainder of the unit. Core 121-753A-2H (10 mbsf) contains 10% micrite. The lower nannofossil ooze at 34.0–43.5 mbsf is notably stiffer and changes in color from pale brown (10YR 7/3 and 10YR 6/4) to white (10YR 8/2) at 37.0 mbsf. Two closely spaced layers of limestone pebbles and pebble fragments are at 43.0 mbsf, near the base of the unit. Whole pebbles are up to 5 cm in diameter (Fig. 4). These pebble layers apparently correlate with the limestone pebble layers observed in sediments at 97 and 105 mbsf in Unit I at Site 752. The pebbly layer contains 10% quartz, which is present throughout the remainder of the unit only in trace amounts. Trace amounts of volcanic glass, opaques, and radiolarians are also present. Individual grains are sand to silt size. The bulk grain size of Unit I ranges from 46 to 96 μm (Table 3 and Fig. 5).

Unit II (43.6–62.8 mbsf) is a calcareous nannofossil with foraminifers chalk sequence. The upper calcareous nannofossil chalk immediately underlying the pebble layer in Unit I consists of a white (10YR 8/2) matrix containing millimeter-scale, light greenish gray (10YR 8/3) planar laminae that are more distinct in the lower part of the unit. The laminae occur in multilayered bundles from 2 to 5 cm thick. The sediment texture is similar to that of the overlying unit, but includes 5% clay-sized grains. Trace amounts of quartz and opaques occur throughout Unit II.

The lower chalk is harder and predominantly white (10YR 8/2) in color, commonly grading into pale yellow (5Y 8/4) zones containing ash layers. The harder chalk contains 6%–10% micrite and 2%–4% siliceous shell material between 53 and 57 mbsf. Sediment texture is similar to that of the overlying chalk, with up to 11% clay-sized grains. Trace amounts of quartz, opaques, and volcanic glass are common.

BIOSTRATIGRAPHY

The main objective at Site 753 was to date the youngest sediment truncated by the unconformity on Broken Ridge. Hole

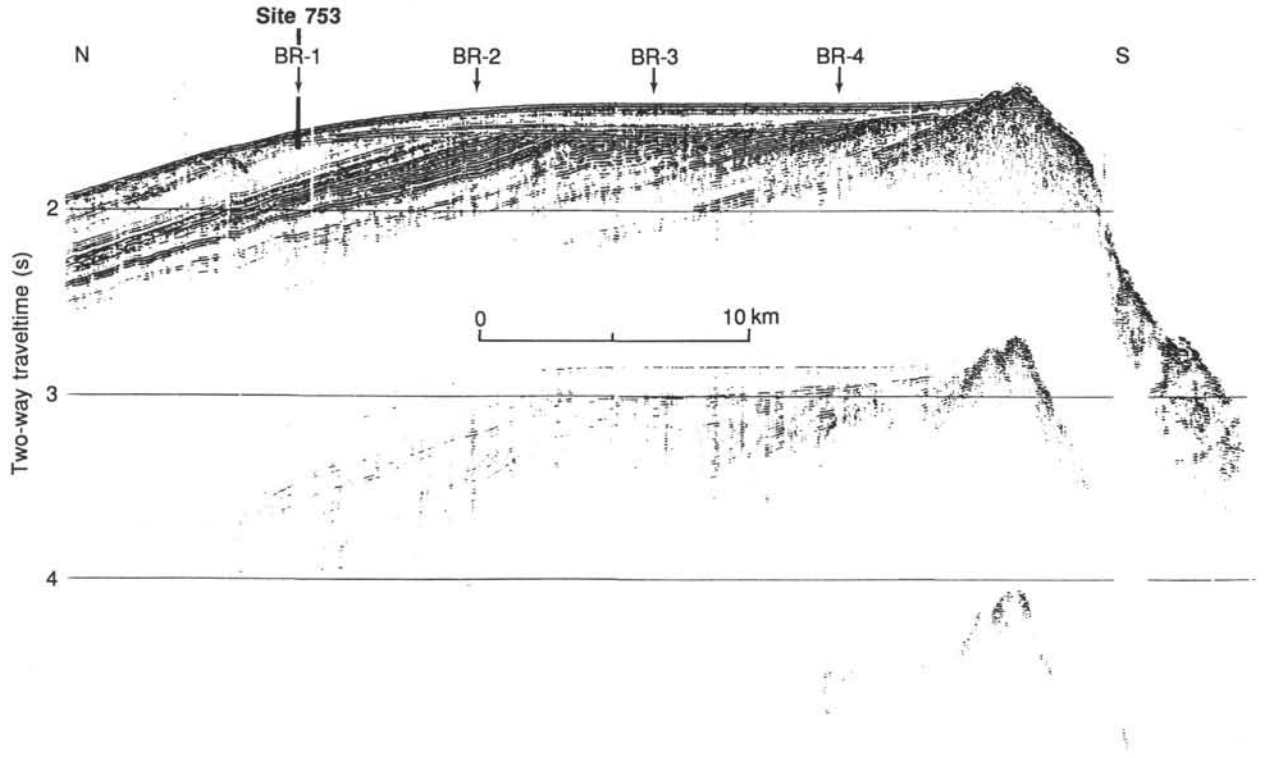

Figure 2. RC2708 single-channel seismic-reflection profile line 20 across Broken Ridge showing Site 753 and proposed Sites BR-1 to BR-4.

Table 1. Coring summary, Site 753.

Core no.	Date (May 1988)	Time (local)	Depth top (mbsf)	Depth bottom (mbsf)	Length cored (m)	Length recovered (m)	Recovery (%)
121-753A-							
1H	12	2035	0.0	7.5	7.5	7.50	100.0
2H	12	2120	7.5	17.2	9.7	8.53	87.9
3H	12	2150	17.2	24.4	7.2	7.48	104.0
4H	13	0005	24.4	34.0	9.6	8.05	83.8
5H	13	0030	34.0	43.6	9.6	9.40	97.9
6H	13	0100	43.6	53.2	9.6	10.05	104.7
7H	13	0305	53.2	62.8	9.6	10.05	104.7
					62.8	61.06	97.2
121-753B-							
1W	13	0845	0.0	24.4	24.4	0.00	0.0
2X	13	0915	24.4	34.0	9.6	0.00	0.0
3W	13	1025	34.0	61.6	27.6	0.05	0.0
4X	13	1100	61.6	71.2	9.6	0.00	0.0
5X	13	1155	71.2	80.9	9.7	0.00	0.0
6X	13	1245	80.9	90.5	9.6	0.03	0.3
7X	13	1340	90.5	100.2	9.7	0.01	0.1
Coring					48.2	0.04	0.1
Washing					52.0	0.05	
					100.2	0.09	

Table 2. Lithologic units at Site 753.

Lithologic unit	Core interval (Hole 753A)	Depth (mbsf)	Lithology
I	1H–5H	0–43.6	Foraminifer/nannofossil ooze
II	6H	43.6–53.2	Nannofossil/calcareous chalk
	7H	53.2–62.8	Nannofossil chalk with foraminifers

753A was drilled to a depth of 62.8 mbsf, and sediments of middle Eocene to Pliocene age were recovered. The condensed Neogene sequence (Cores 121-753A-1H to 121-753A-5H) consists of foraminifer/nannofossil ooze and may be confirmed by further detailed biostratigraphic study as complete. The nannofossil chalks directly below the unconformity, in Cores 121-753A-6H and 121-753A-7H, are dated as middle Eocene and placed in nannofossil Zone CP13c and planktonic foraminifer Zones P10–12. Figure 6 is a summary of the age-depth relationship drawn from the datum levels in Table 4. The biostratigraphic results are summarized in Figure 7.

Recovery from Hole 753A was nearly perfect, in contrast to the 0.1% recovery in Hole 753B. The Neogene section was washed through in Hole 753B, and XCB coring commenced at 61.6 mbsf and terminated at 100.2 mbsf. Problems with the hinge pin holding the flapper of the float valve caused blockage of the core barrel, resulting in the minuscule recovery. The bits of sediment recovered from this hole were dated as middle Eocene, but considering the problems during coring, age-depth relationships cannot be certain.

Calcareous nannofossils are abundant in all cores, with good preservation in the Pliocene and the middle Eocene sediments. Strong overgrowth of the discoasters, combined with the lack of zonal markers because of latitudinal effects, made zonal assignments of the lower and middle Miocene sections more difficult. Similar problems were encountered in the Miocene sections by the planktonic foraminiferal paleontologists. Neogene planktonic foraminifers are abundant and well preserved, with assemblages showing Southern Ocean, mid-latitude affinities. The Eocene planktonic foraminifer assemblages are of a temperate nature.

Benthic foraminifers are rare in the upper sections of the Neogene, but common, well-preserved specimens were found in the middle Eocene cores, as well as in the lower and middle

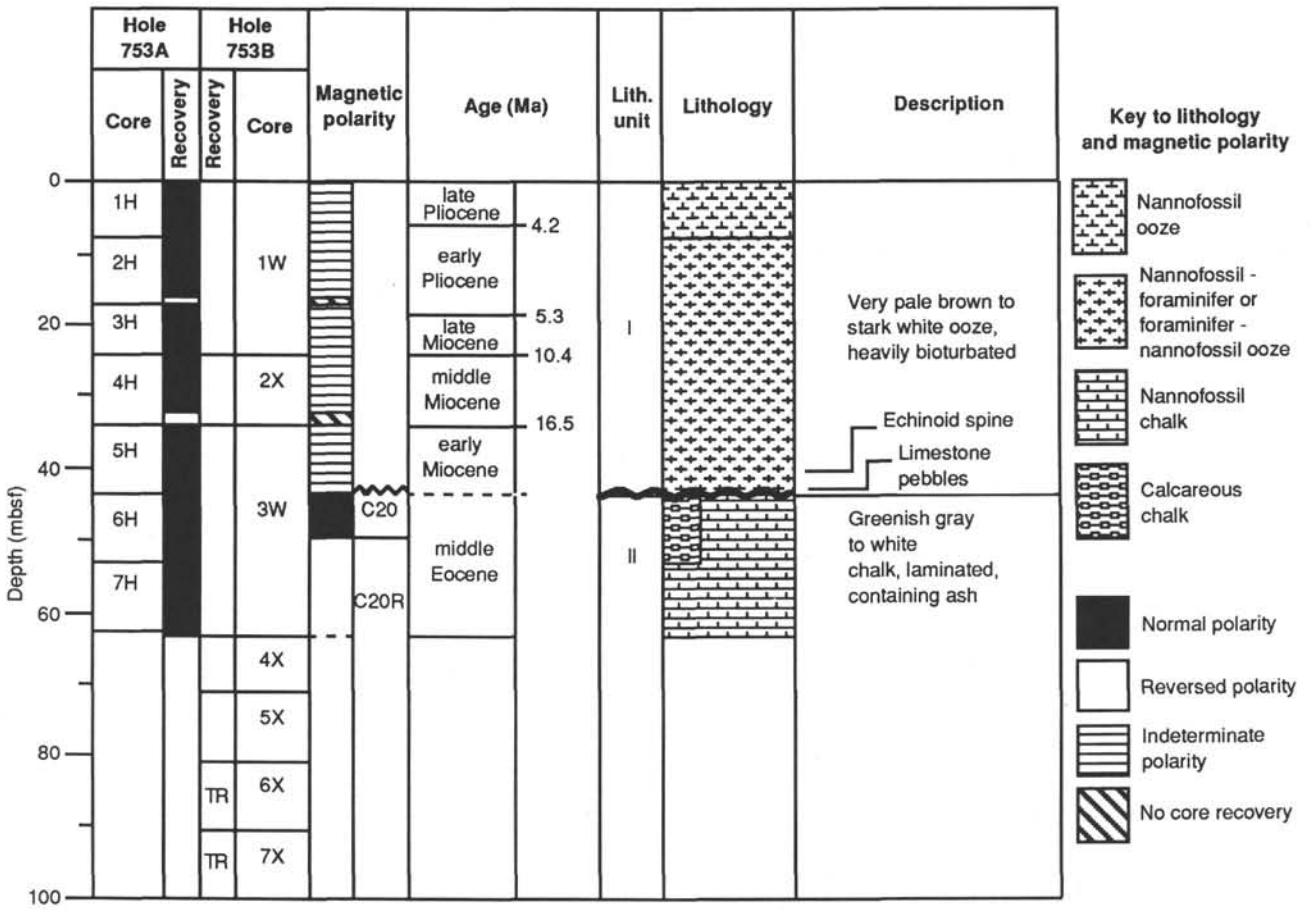

Figure 3. Site 753 summary diagram.

Miocene sequences. Water depths in the Neogene are indicated by benthic foraminifers to be middle to lower bathyal. Lower bathyal water depths were determined from the middle Eocene assemblages.

Abundant, well-preserved diatoms are present only in the Eocene sediments. In addition to the diatoms are radiolarians, silicoflagellates, and sponge spicules. The presence of abundant siliceous microfossils may be a good indicator of high productivity and is an important aspect in paleoceanographic interpretations. In addition, diatom- and radiolarian-rich Paleogene sediments from Sites 752 and 753 offer an excellent opportunity for biostratigraphic integrations with the calcareous microfossil groups.

Calcareous Nannofossils

Calcareous nannofossils are generally abundant in all the sediments recovered at Site 753. Preservation is moderate in most samples and good in Samples 121-753A-6H-CC and 121-753A-7H-CC.

The low-latitude zonation scheme of Okada and Bukry (1980) was successfully applied for the Pliocene-Pleistocene sediments at Hole 753A, but we encountered difficulties in the Miocene sections because of the high latitudinal nature of the nannofossil assemblages.

Neogene

The first five cores recovered from Hole 753A contain a condensed Neogene sequence, which may be complete. Sections 121-753A-1H-1 through 121-753A-1H-5 are assigned a Pliocene age. Discoasters are common and moderately to well preserved. Pleistocene sediments were not noted and may occur only near the top of Core 121-753A-1H. The last occurrence of *Reticulofenestra pseudoumbilica* in Sample 121-753A-1H-4, 47–48 cm (4.97–4.98 mbsf), coincides with the base of Zone CN12 of Okada and Bukry (1980). The last occurrence of *Amaurolithus primus* is noted in Sample 121-753A-1H-5, 47–48 cm (6.47–6.48 mbsf), marking the base of Zone CN11.

Sample 121-753A-1H-CC (7.5 mbsf) contains a moderately well-preserved assemblage that includes *Amaurolithus tricorniculatus, A. primus, Amaurolithus delicatus, Ceratolithus acutus*, and *Ceratolithus rugosus*. This assemblage is representative for the lower Pliocene and is assigned to Zone CN10b. The first occurrence of *C. acutus*, in Sample 121-753A-2H-4, 47–48 cm (12.47–12.48 mbsf), is used here to approximate the Miocene/Pliocene boundary. The first occurrence of this form has been observed just above the Miocene/Pliocene boundary in Capo, Rossello, the Zanclean Stratotype in Sicily (Perch-Nielsen, 1985).

The first occurrence of *Discoaster surculus*, in Sample 121-753A-2H-6, 47–48 cm, is used to mark the base of Zone CN9. The nannofossil assemblage consisting primarily of *Discoaster pentaradiatus, Discoaster surculus*, and *R. pseudoumbilica* in Samples 121-753A-2H-CC (17.2 mbsf) and 121-753A-3H-CC (24.4 mbsf) is considered to be late Miocene (CN8) in age. The appearance of *Sphenolithus heteromorphus* together with *Discoaster deflandrei* in Sample 121-753A-4H-CC (34.0 mbsf) is indicative of Zone CN4. Sample 121-753A-5H-CC (43.6 mbsf), in the interval just above the hardground, contains *Cyclicargolithus abisectus* and *D. deflandrei* and is lower Miocene/uppermost Oligocene (CN1–2). A few reworked Eocene and Oligocene fossils, such as *Chiasmolithus solitus, Zygrhabdolithus bi-*

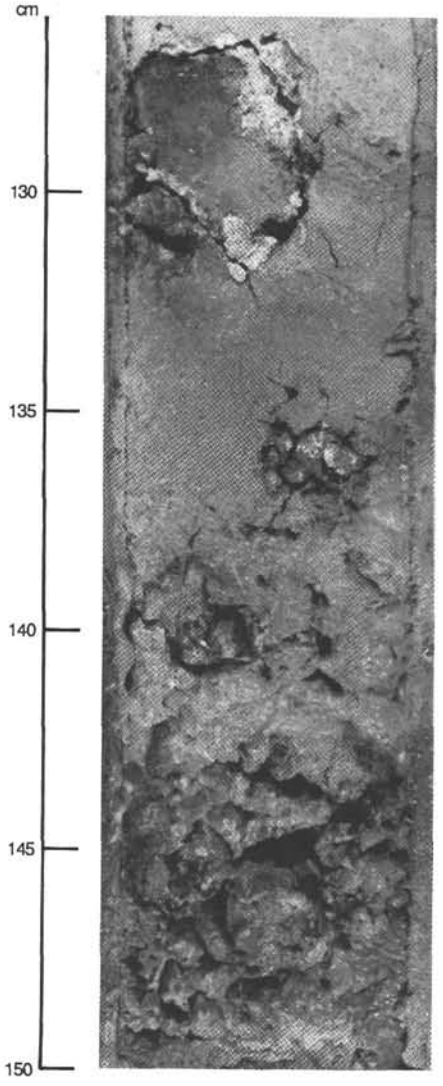

Figure 4. Limestone pebble layer (Section 121-753A-5H-6, 126–150 cm).

Table 3. Grain-size data for Hole 753A sediments.

Core, section, interval (cm)	Depth (mbsf)	Mean grain size (μm)	(ϕ)
Lithologic Unit I			
1H-2, 80	2.3	51.5	4.30
1H-CC, 1	7.5	60.0	4.05
2H-2, 80	9.8	58.9	4.10
2H-CC, 1	17.1	76.8	3.70
3H-2, 80	19.5	45.7	4.45
3H-CC, 1	24.3	47.2	4.40
4H-2, 80	26.7	30.6	5.10
4H-CC, 1	33.9	68.3	3.85
5H-2, 80	36.3	96.4	3.35
5H-CC, 1	43.5	53.8	4.20
Lithologic Unit II			
6H-2, 82	45.9	16.8	5.90
6H-CC, 1	53.1	35.8	4.85
7H-2, 80	55.5	22.1	5.50

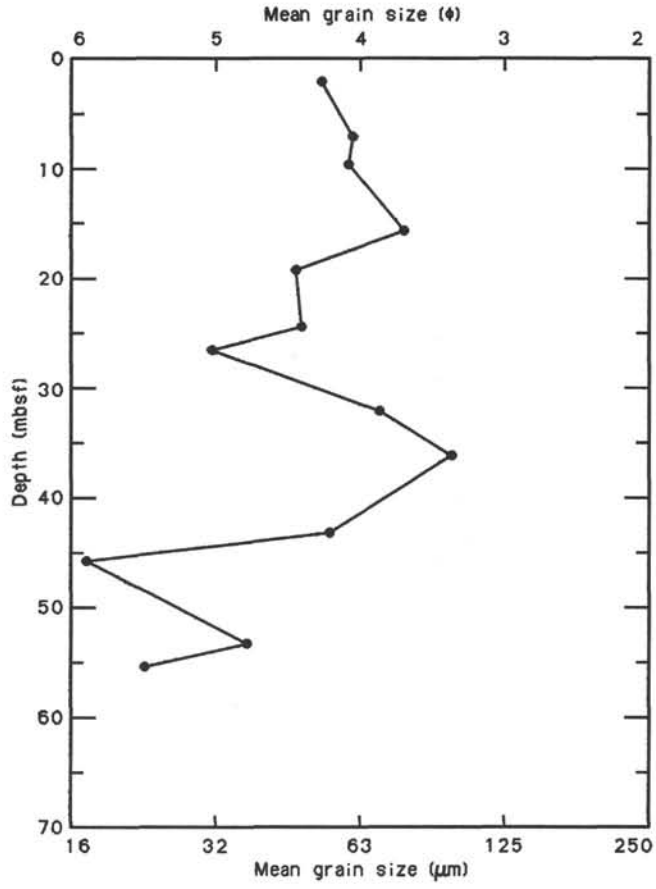

Figure 5. Mean grain size of the bulk sediment at Site 753.

jugatus, and *Tribrachiatus orthostylus*, were found in the Miocene section.

The subdivisions of the Miocene are based mainly on discoasters, which makes zonation at Site 753 difficult because few of these species have been recognized. The absence of these warm-water species is indicative of the midlatitude location of Broken Ridge.

Paleogene

The diverse assemblage of calcareous nannofossils from Cores 121-753A-6H and 121-753B-7H (53.2 and 62.8 mbsf, respectively) is middle Eocene (Zone CP13c). Species of *Nannotetrina* are present, along with *C. solitus, Chiasmolithus grandis, Discoaster saipanensis*, and *Discoaster barbadiensis*. Mechanical problems limited the recovery in Hole 753B. Core 121-753B-3W (61.6 mbsf) contains an assemblage similar to that in Cores 121-753B-6H and 121-753B-7H and is assigned to Zone CP13c. Core 121-753B-5X (80.9 mbsf) is assigned to Zone CP13b, based on the presence of the subzonal marker *Chiasmolithus gigas*.

In summary, the unconformity present on Broken Ridge between lower Miocene sediments and middle Eocene sediments is well constrained. Zones CP14 through CP19 (late Eocene and Oligocene age) are missing at this site, but the Neogene section at Site 753 may be complete. Several nannofossil biostratigraphic zones are combined in the Miocene section because of the lack of marker species resulting from the high latitudinal nature of the nannofossil assemblages.

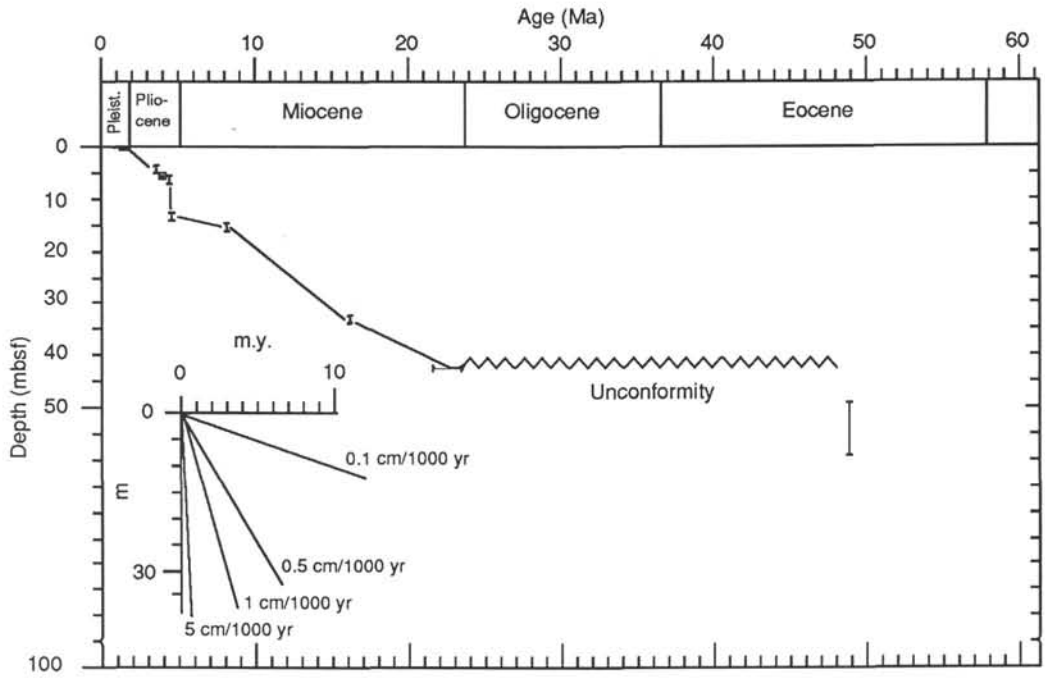

Figure 6. Age vs. depth plot for Site 753.

Table 4. Datum levels used in Hole 753A.

Species[a]	Age (Ma)	Depth (mbsf)
Planktonic foraminifers		
FO *Globorotalia inflata*	3.0	4.5
FO *Globorotalia crassaformis*	4.1	6.0
FO *Globorotalia puncticulata*	4.4	7.5
LO *Globorotalia mayeri*	10.4	17.2
FO *Orbulina* spp.	15.2	34.4
FO *Globigerinoides*	23.3	43.6
LO *Globigerina primitiva*	42.8	43.6
FO *Globigerinatheka subconglobata*	49.0	62.6
Calcareous nannofossils		
LO *Discoaster brouweri*	1.9	1.0
LO *Reticulofenestra pseudoumbilica*	3.5	4.97
LO *Amaurolithus primus*	4.4	6.47
FO *Ceratolithus acutus*	4.5	12.5
FO *Discoaster surculus*	8.2	14.5
LO *Discoaster deflandrei*	16.2	34.0
LO *Chiasmolithus gigas*	47.0	62.8

[a] FO = first occurrence; LO = last occurrence.

Planktonic Foraminifers

Samples 121-753A-1H-CC to 121-753A-5H-CC contain a condensed Neogene sequence that is almost complete. At the base of this sequence in Sample 121-753A-5H-CC, a late Oligocene to earliest Miocene age assemblage of planktonic foraminifers occurs above and within the hardground. Below the hardground in Sample 121-753A-6H, 10–11 cm, is a middle Eocene assemblage of planktonic foraminifers, which extends down to Sample 121-753A-7H-CC.

Neogene

A well-preserved Neogene assemblage of planktonic foraminifers was recovered down to 43.6 mbsf. In contrast, the planktonic foraminiferal assemblages within and below the hardground are recrystallized and overgrown with calcite.

Dominating the Neogene assemblages are typical, high-latitude, temperate faunas and other more cosmopolitan species. The recovered faunas have an affinity with other Neogene faunas at midlatitudes in the Southern Hemisphere, for example, southeast Australia (Jenkins, 1960), New Zealand (Jenkins, 1967, 1971), the South Atlantic (Jenkins, 1978), and the South Pacific (Kennett, 1973). Significantly, *Globigerina bulloides*, which is restricted to transitional and cooler waters at the present (Bé and Tolderlund, 1971), is found in abundance throughout.

The lack of low-latitude marker species prevents application of the tropical zonation schemes proposed by Banner and Blow (1965), Blow (1969), or Bolli et al. (1985). Instead, the higher latitude zonal schemes of Srinivasan and Kennett (1981) and Kennett (1973) were applied to sediments of early to middle Miocene and late Miocene to Holocene ages, respectively.

No Pleistocene sediments were recovered.

Pliocene

A complete Pliocene sequence of sediments was recovered from Samples 121-753A-1H-1, 90–96 cm, through 121-753A-2H-1, 144–146 cm. Four zones were delineated in the Pliocene, based on the first occurrence of *Globorotalia puncticulata, Globorotalia crassaformis, Globorotalia inflata*, and *Globorotalia tosaensis*. In the Pliocene sediments, temperate species such as *G. bulloides, Globigerina falconensis, Globigerina woodi, Globorotalia conoidea, Globorotalia conomiozea, G. puncticulata*, and *G. inflata* dominate the assemblages, alongside the more cosmopolitan species *Orbulina universa, Orbulina suturalis*, and *Globorotalia margaritae*. Pliocene warm- to tropical-water forms such as *Globorotalia tumida, Globorotalia tumida flexuosa, Sphaeroidinella dehiscens, Pulleniatina obliquiloculata, Pulleniatina primalis, Globigerinoides fistulosus, Neogloboquadrina humerosa*, and *Neogloboquadrina dutertrei* are absent.

Miocene

A possible continuous Miocene sedimentary sequence was recovered from Samples 121-753A-2H-3, 149–151 cm, to 121-753A-5H-CC. As in the Pliocene section, the planktonic foraminifer assemblage is dominated by *G. bulloides* and *G. woodi*.

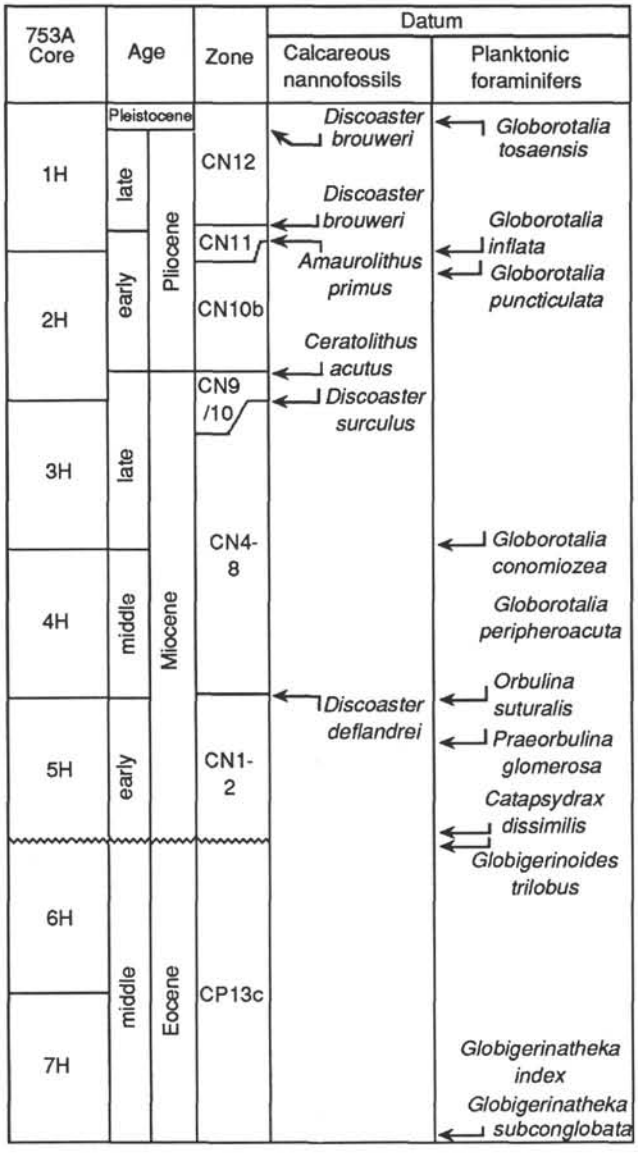

Figure 7. Biostratigraphic results of Site 753. Ages are from Bolli et al. (1985).

The Miocene/Pliocene boundary was tentatively placed at the evolutionary appearances of *G. puncticulata* and *G. margaritae*, in Sample 121-753A-2H-1, 144–146 cm.

The base of the upper Miocene was delineated by the last appearance of *Globorotalia mayeri*. Within the upper Miocene assemblages there is an abundance of *Globigerina nepenthes, G. conoidea, Globorotalia miozea, Globorotalia panda*, and *Globoquadrina dehiscens*.

The base of the middle Miocene was delineated on the first appearance of *O. suturalis* from *Praeorbulina glomerosa curva* (the *Orbulina* datum), at Sample 121-753A-4H-CC. All three planktonic foraminiferal zones in the middle Miocene were discerned. The absence of the low-latitude marker species *Globorotalia praefohsi, Globorotalia fohsi, Globorotalia fohsi lobata*, and *Globorotalia fohsi robusta* testifies to the higher latitudinal position of Broken Ridge in the Miocene. Only the more temperate to subtropical earlier forms of the *G. fohsi* evolutionary lineage, *Globorotalia peripheroronda* and *Globorotalia peripheroacuta*, were found. The co-occurrence of these two forms in Samples 121-753A-4H-1, 100–105 cm, to 121-753A-4H-4, 100–105 cm, delineates the *Globorotalia peripheroronda–Globorotalia peripheroacuta* Zone of the middle Miocene.

The top of the lower Miocene, the *Praeorbulina glomerosa* Zone, is represented in Samples 121-753A-5H-1, 10–11 cm, to 121-753A-5H-1, 10–11 cm. Within this interval the ancestral forms of *Orbulina—Praeorbulina sicana, Praeorbulina glomerosa curva, Praeorbulina glomerosa glomerosa*, and *Praeorbulina glomerosa circularis*—are present.

Below this interval down to Sample 121-753A-5H-CC, the sediments are of early Miocene age, characterized by *G. dehiscens, Globigerinoides trilobus, Catapsydrax dissimilis, G. bulloides, Globorotalia incognita*, and *Globorotalia zealandica*. In Sample 121-753A-5H-CC, sediments assigned to the *Globigerinoides trilobus* Zone contain a reworked, poorly preserved assemblage of upper Eocene forms such as *Hantkenina* sp., *Globorotalia cerroazulensis, Acarinina*, and *Truncorotaloides*.

Paleogene

Preliminary analysis of the assemblages at 80.9 mbsf in Sample 121-753B-5X-CC shows the presence of three distinct faunas. The first fauna contains relatively rare specimens of *G. trilobus* and is of early Miocene age. The second fauna is of Late Cretaceous to early/middle Eocene age, which is clearly reworked from strata of this age recovered at Sites 752 and 754, where identical assemblages were found. This second fauna is represented by *Globigerinatheka index, Globigerinatheka subconglobata, Acarinina bullbrooki, Acarinina primitiva*, and a few Cretaceous *Globigerinelloides*. The third fauna is of late Eocene and late Oligocene age, with well-preserved specimens, although we observed signs of dissolution with the scanning electron microscope and many of the tests were broken. *Globigerina selli, Globigerina tripartita, Globorotalia increbescens, Globorotalia euapertura, Globigerina eocaena, Globigerina gortanii, Globigerina angiporoides, Globorotalia* aff. *centralis, G. cerroazulensis, Chiloguembelina cubensis*, and *Hantkenina* sp. form this third assemblage.

The third assemblage may have important implications, because it indicates that pelagic sedimentation at the southern part of Broken Ridge continued from the late Eocene to the late Oligocene, possibly with an interruption resulting from a late Oligocene eustatic sea-level low stand that removed lower Oligocene strata. The upper Oligocene to lower Miocene chert gravel-rich lag may represent the final rise above sea level at Site 753. Section 121-753A-5H-CC is within this chert gravel lag and contains a reworked pelagic fauna from nearby Eocene to Oligocene strata.

A temperate assemblage is found from 80.9 to 100.2 mbsf (Samples 121-753B-6X-1, 10–11 cm, to 121-753B-7X-CC), the bottom of Hole 753B. The faunas are dominated by *A. primitiva* and *A. bullbrooki*, with low numbers of index species such as *G. index* and *G. subconglobata*. These index species indicate the middle Eocene age *Globigerinatheka index* Zone of Jenkins (1985). The austral temperate zonation established by Jenkins (1985) proved useful because most of the typical low-latitude marker species were missing throughout the Paleogene. This *G. index* Zone is comparable to the low-latitude *Globigerinatheka subconglobata* to *Truncorotaloides rohri* Zones (P11–14) (Toumarkine and Luterbacher, 1985; Bolli et al., 1985).

All of the faunas are indicative of a cool, temperate climate because most low-latitude markers are missing. The planktonic/benthic ratio is high (>90/10) in the Paleogene assemblages, indicating water depths in excess of 400 m.

Benthic Foraminifers

Benthic foraminifers (>125 μm) were examined from all core-catcher samples recovered in Holes 753A and 753B. The preser-

vation of benthic foraminifers is good, although they are rare in the planktonic foraminiferal ooze.

Pliocene to Miocene

The Pliocene to lower Miocene faunas (Samples 121-753A-1H-CC to 121-753A-5H-CC) are dominated by *Laticarinina pauperata, Ehrenbergina carinata, Cibicidoides kullenbergi, Planulina wuellerstorfi, Pullenia bulloides, Oridorsalis umbonatus, Stilostomella*, and *Orthomorphina*. These faunal characters indicate lower bathyal depths during the Pliocene to Miocene.

The faunal associations consisting of abundant *Globocassidulina subglobosa* in the Pliocene sediments and several smaller globocassidulinid faunas associated with *P. bulloides* and *P. wuellerstorfi* in the Miocene indicate that the bottom water masses were related to Indian Deep Water.

Eocene

The middle Eocene faunas are composed of *Anomalinoides capita, Cibicidoides* spp., and *Planulina* spp. *Stilostomella*, and *Orthomorphina* are commonly found. *Nuttalides truempyi*, the most typical element in the Eocene, is consistently present—but not abundant—at this site. The aforementioned taxa, plus *Osangularia mexicana*, indicate a lower bathyal depth.

Diatoms

Diatoms were found only in the Eocene sediments. The diatom stratigraphy used here is that of Fenner (1984).

Hole 753A

Diatoms occur only in Core 121-753A-7H. The assemblages are moderately preserved and are dominated by species belonging to the genera *Hemiaulus, Stephanopyxis*, and *Triceratium*. *Melosira architecturalis* and *Triceratium inconspicuum* var. *trilobata* in Sample 121-753A-7H-3, 55–57 cm, indicate a middle Eocene age.

Hole 753B

In Hole 753B, only 3 cm was recovered in Core 121-753B-6X and 1 cm in Core 121-753B-7X. Diatoms are abundant and well preserved in samples from these cores. The assemblages are similar at these two levels and are dominated by the genera *Triceratium, Hemiaulus, Coscinodiscus, Melosira*, and *Stephanopyxis*. The occurrence of *Trinacria excavata* forma *tetragona, T. inconspicuum* var. *trilobata, Triceratium kanayae, Skeletonema barbadense, M. architecturalis*, and *Rylandsia biradiata* allows the assignment of this interval to the middle Eocene.

Other Siliceous Microfossils

Radiolarians, silicoflagellates, and sponge spicules are abundant and well preserved at the same levels as the diatoms.

PALEOMAGNETICS

Paleomagnetic analysis of sediments from Hole 753A consisted primarily of whole-core susceptibility and remanence measurements. No measurements were made on the small amount of material recovered from Hole 753B. Alternating field (AF) demagnetization of discrete samples in peak values above 8 mT was limited to four samples from the middle Eocene sequence (121-753A-6H-1, 65–67 cm, 121-753A-6H-2, 63–65 cm, 121-753A-6H-7, 57–59 cm, and 121-753A-7H-6, 61–63 cm). The results show that AF demagnetization above 20 mT may be necessary to remove overprints. The magnetostratigraphic interpretation, therefore, is preliminary and may be revised significantly after shorebased analysis.

Susceptibility

The bulk magnetic susceptibility of the Neogene cap (the interval from Core 121-753A-1H to 43 cm in Core 121-753A-5H) is weak; this interval is probably dominated by either paramagnetic or diamagnetic minerals. Values range from -1×10^{-6} to 1×10^{-5} cgs units, with most in the range of 10^{-6} cgs units. The Miocene/middle Eocene unconformity at the top of Core 121-753A-6H (43.6 mbsf) is clearly visible on the susceptibility plot (Fig. 8). Below the unconformity, the susceptibilities are all positive with values predominantly in the range of 10^{-5} cgs units and spikes as high as 2×10^{-4} cgs units. The middle Eocene sequence does not show the characteristic pattern of sudden increases/gradual decreases in susceptibility that was observed in the lower Eocene to middle Paleocene sequence from Hole 752A.

Remanence

The initial intensity of the natural remanent magnetization (NRM) of the Miocene-Pliocene sequence increased downcore, ranging from 1×10^{-1} to 5 mA/m. In general, the lower intensities were below or at the noise level of the cryogenic magnetometer. Below the unconformity, the initial NRM intensity of the middle Eocene sequence was around 10 mA/m, decreasing to 1 mA/m at the base of the recovered sequence.

Comparison of initial NRM results with results after AF demagnetization at 8 mT suggests a tentative polarity pattern for the Miocene-Pliocene sequence (Fig. 9). Because of the weak magnetization, this pattern needs to be confirmed by discrete sample demagnetization studies at higher peak AF values. Detailed biostratigraphic control is not available at this time. Accordingly, no attempt has been made to correlate this tentative reversal pattern with the Berggren et al. (1985) scheme.

For the middle Eocene sequence, whole-core demagnetization at 8 mT had only a minimal effect on magnetization direc-

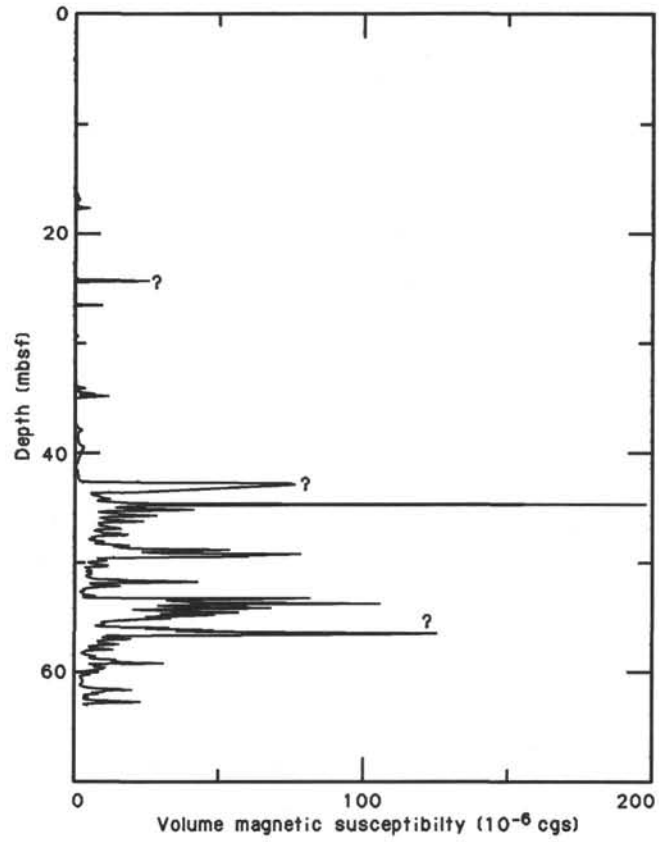

Figure 8. Whole-core susceptibility data for Hole 753A. Large single-measurement peaks (labeled with question marks) at the core tops probably represent rust contamination.

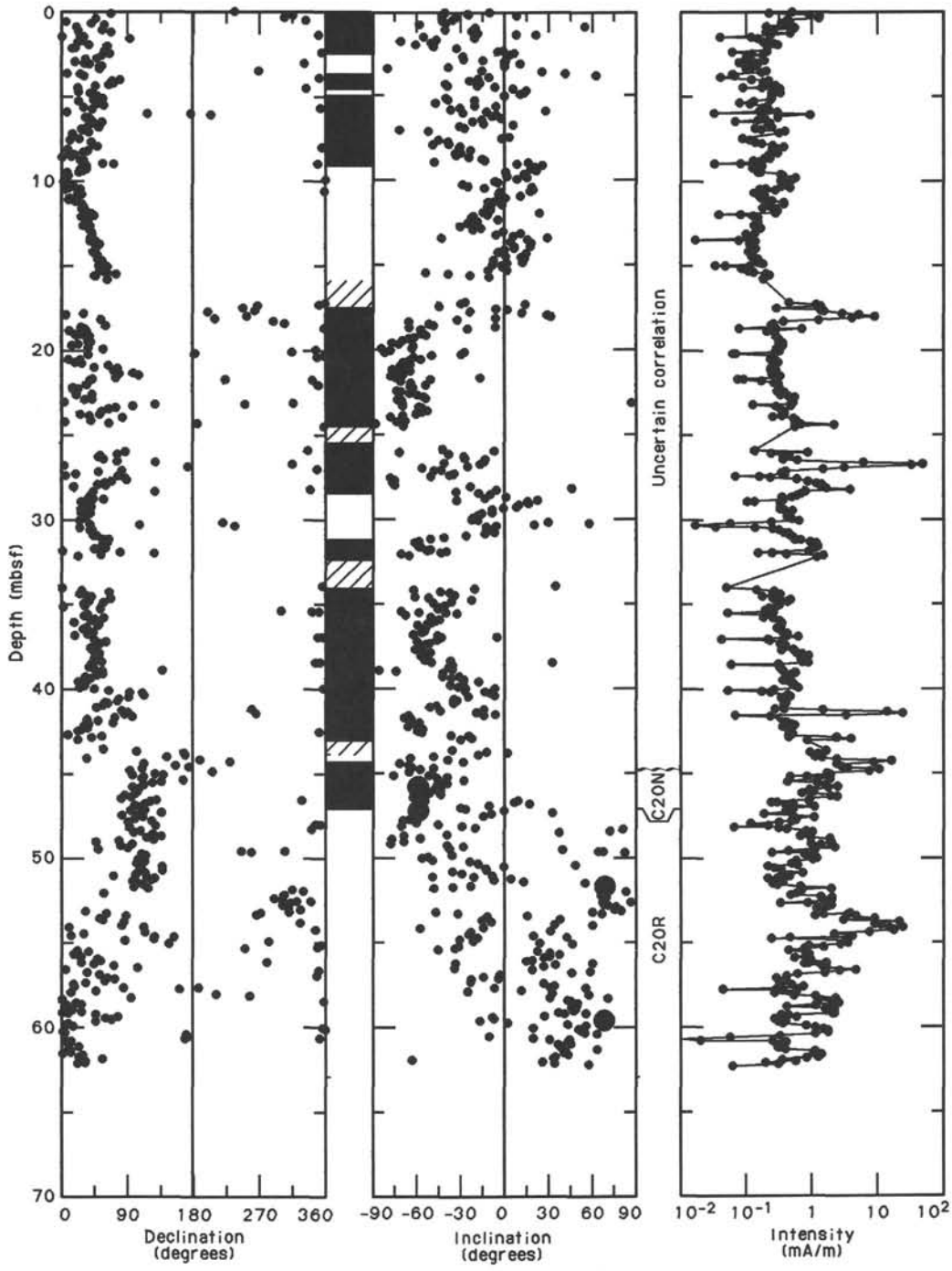

Figure 9. Whole-core remanence data for Hole 753A after 8-mT demagnetization and preliminary correlation with the Berggren et al. (1985) geomagnetic reversal time scale. Black is normal polarity; diagonal line pattern indicates no recovery. Large dots on the inclination diagram indicate results from discrete sample demagnetization studies.

tions. The whole-core results suggest a normal polarity interval from the Miocene/middle Eocene unconformity (43.6 mbsf) down to 46.5 mbsf, which is followed by a reversed polarity interval to the base of the recovered sequence (62.8 mbsf). The normal polarity interval is identified as Chron C20N, assuming the presence of calcareous nannofossil Zone CP14. The reversed polarity interval is assigned to Chron C20R, based on the presence of calcareous nannofossil Zone CP13c. The polarity interpretation is confirmed by demagnetization studies of four discrete samples from Cores 121-753A-6X and 121-753A-7X (Figs. 10 and 11). These samples showed a rather soft magnetization (median demagnetizing fields around 10 mT), but no indication of major overprints.

The probable presence of overprints in the whole-core data (for which a proper deconvolution procedure is not available at this time) and the contamination of discrete samples by the DC

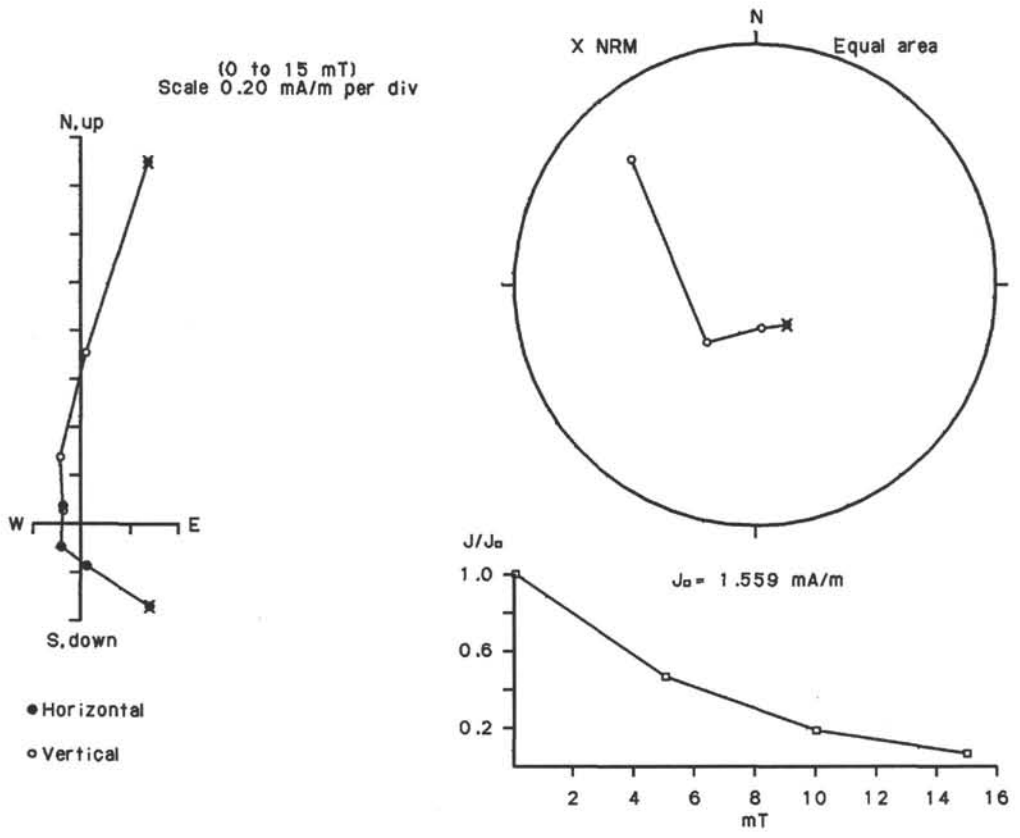

Figure 10. Zijderveld, equal area, and intensity decay plots for Sample 121-753A-6H-1, 65–67 cm, indicate normal polarity (with Chron C20N) for the top part of the recovered middle Eocene sequence. The lack of convergence on the origin is probably due to the Schonstedt demagnetizer's DC bias, which becomes appreciable at alternating fields in excess of 10–15 mT.

bias of the Schonstedt AF demagnetizer prevent the reliable estimate of paleolatitude. Shorebased studies are necessary for this determination.

INORGANIC GEOCHEMISTRY

The objectives of the inorganic geochemistry studies for Leg 121 are given in the "Inorganic Geochemistry" section of the "Site 752" chapter. A summary of the overall results of Leg 121 for Broken Ridge is presented in the "Broken Ridge Summary" chapter (this volume).

Discussion of Results

The interstitial-water chemical analyses are listed in Table 5. The calcium and magnesium concentrations in the pore waters closely match those at Site 752 (see "Inorganic Geochemistry" section, "Site 752" chapter). The alkalinities and sulfate concentrations also match those of Site 752. Samples at Site 753 were obtained only to a depth of 60 mbsf, so it is impossible to say if the chemical match continues at greater depths. Assuming that the relationship between Sites 752 and 753 holds, a comparison can be made between the two. The amount of alteration of volcanic material either in the sediments or basement at the two sites is similar, as is the low degree of sulfate reduction and oxidation of organic matter in the sediments. In view of the fact that the two sites are only 3 km apart, these similarities seem reasonable. The sites differ in that Site 753 has a thinner Neogene sediment cap and slightly younger sediments below the unconformity. Apparently these differences are not enough to make a noticeable difference in the pore-water chemistry.

ORGANIC GEOCHEMISTRY

Few gas analyses and carbonate carbon analyses were performed on the physical-properties samples from Site 753. A detailed description of the methods used is in the "Explanatory Notes" chapter (this volume). Because of the low contents of organic matter in the sediments from Site 752, no measurements of organic carbon percentages and no Rock-Eval pyrolyses were performed at Site 753.

Gas Analyses

Headspace gas analyses from Cores 121-753A-4H and 121-753A-7H found methane concentrations of 122 and 6 ppm, respectively (122 ppm is equivalent to 400 μL methane/L sediment). Ethane and propane were not detected.

Carbonate Content

Sediment samples from Hole 753A are similar to those from Hole 752A in that they are rich in carbonate (Table 6). Sediments from the upper 40 m consist of fairly pure carbonate (Fig. 12). This lithologically homogeneous interval (see "Lithostratigraphy and Sedimentology" section, this chapter) includes sediments of Pliocene, as well as late and early Miocene, age. They are underlain by middle Eocene sediments that have slightly lower and more variable carbonate percentages than those in the Neogene.

PHYSICAL PROPERTIES

The sediments cored at Site 753 are a condensed Pliocene to Eocene sequence composed of carbonate ooze and chalk with

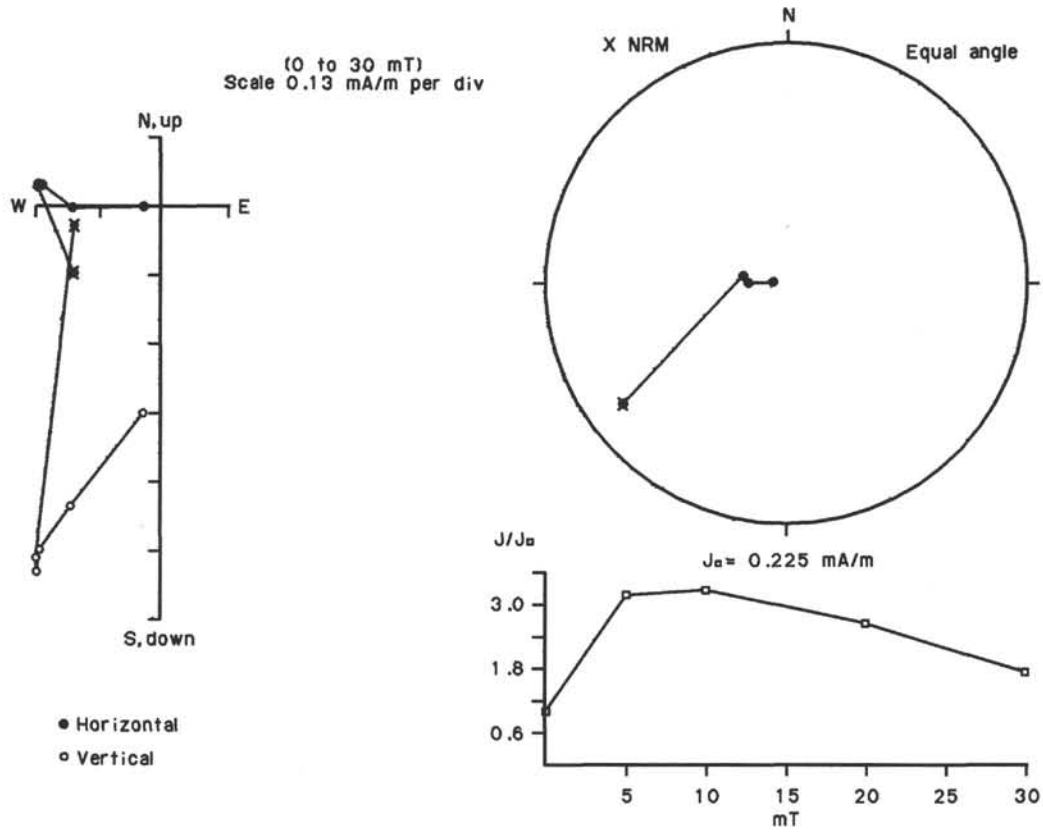

Figure 11. Zijderveld, equal area, and intensity decay plots for Sample 121-753A-6H-7, 57–59 cm, indicate reversed polarity (Chron C20R) for the middle and basal part of the recovered middle Eocene sequence.

Table 5. Interstitial-water geochemistry data, Hole 753A.

Core, section, interval (cm)	Depth (mbsf)	Volume (mL)	pH	Alkalinity (mmol/L)	Salinity (g/kg)	Magnesium (mmol/L)	Calcium (mmol/L)	Chloride (mmol/L)	Sulfate (mmol/L)
1H-4, 145–150	6.0	35	7.6	2.71	35.0	52.7	11.1	559	29.5
[a]4H-1, 0–1	24.4	14	7.9	2.72	35.5	50.0	13.5	563	29.0
4H-4, 145–150	30.4	44	7.7	2.58	35.5	50.0	13.3	556	29.5
[a]7H-1, 0–1	53.2	11			35.5	45.5	15.1	561	29.5
7H-5, 145–150	60.7	40	7.7	2.30	36.0	47.9	15.4	562	29.5

[a] Sampled by the Barnes *in-situ* water sampler.

green laminae. A pebble layer above the chalks represents a hiatus between lower Miocene and middle Eocene sediment. The sediments in Cores 121-753A-1H to 121-753A-5H were deposited in a middle to lower bathyal environment and the sediments in Cores 121-753A-6H to 121-753A-7H in a lower bathyal environment. Hole 753A was cored with the APC, which is commonly used in such softer sediments and does not disturb a sedimentary sequence as much as the rotary coring method. The samples tested are judged to be of fairly good quality for physical-properties measurements, improving toward the base of the section.

Methods

Sediments from this site were measured for index properties (pycnometer and balance and GRAPE), compressional-wave velocity (*P*-wave logger), vane shear strength, electric resistivity, and thermal conductivity. Descriptions of these methods are found in the "Explanatory Notes" chapter.

Results

Index Properties

Porosity, bulk density, water content (expressed as water weight relative to wet sample weight), grain (or matrix) density, and dry-bulk density of the Site 753 sediments are listed in Table 7 and plotted relative to depth in Figure 13. Sediments recovered from this short hole vary little in their index properties. Porosity ranges between 60% and 65%, and bulk density is between 1.6 and 1.7 g/cm^3, except for the interval at 36–43 mbsf where the values are slightly lower (between 1.5 and 1.6 g/cm^3). This latter section corresponds to the lower Miocene ooze immediately above the pebble layer. Water content gradually decreases from 40% at the surface to <35% at the base of Hole 753A. These values represent much lower water contents than expected in most calcareous sediments. The slight water content increase about 36–43 mbsf mirrors the decrease in the bulk density. The grain density is stable at about 2.7 g/cm^3, and dry-bulk density values are approximately 1 g/cm^3.

Table 6. Percentages of inorganic carbon and calcium carbonate in samples from Hole 753A.

Core, section, interval (cm)	Depth (mbsf)	Inorganic carbon (%)	Calcium carbonate (%)
1H-2, 80–82	2.30	11.62	96.8
1H-4, 80–82	5.30	11.56	96.3
2H-2, 80–82	9.80	11.69	97.4
2H-4, 80–82	12.80	11.75	97.9
2H-6, 80–82	15.80	11.60	96.6
3H-2, 80–82	19.50	11.53	96.0
3H-4, 80–82	22.50	11.42	95.1
4H-2, 80–82	26.70	11.63	96.9
4H-4, 80–82	29.70	11.60	96.6
5H-2, 80–82	36.30	11.47	95.6
5H-4, 80–82	39.30	11.45	95.4
5H-6, 80–82	42.30	10.89	90.7
6H-2, 82–84	45.92	11.09	92.4
6H-4, 80–82	48.90	10.58	88.1
6H-6, 80–82	51.90	9.99	83.2
7H-2, 80–82	55.50	10.94	91.1
7H-4, 80–82	58.50	10.88	90.6
7H-6, 80–82	61.50	10.57	88.1

Compressional-Wave Velocity

Velocity data collected by the *P*-wave logger are displayed in Figure 13. Velocities range between 1500 and 1600 m/s throughout the sediment column. The impedance log computed from GRAPE and *P*-wave-logger data shows several slight impedance contrasts, which can be considered as possible sources of reflected seismic energy for the section (see "Seismic Stratigraphy" section, this chapter). Almost all of the impedance contrasts are caused solely by increases in seismic velocity.

Vane Shear Strength

Records of undrained shear strengths were obtained from Hole 753A sediments (Table 7 and Fig. 13). The shear strength of the ooze is very low (0–12.6 kPa), but increases markedly with the lithology change between ooze and chalk at about 45 mbsf to over 100 kPa. Shear strengths decrease from this high value to about 60 kPa.

Formation Factor

The formation factor is measured by comparing the electrical resistance of a sediment against the resistance of seawater.

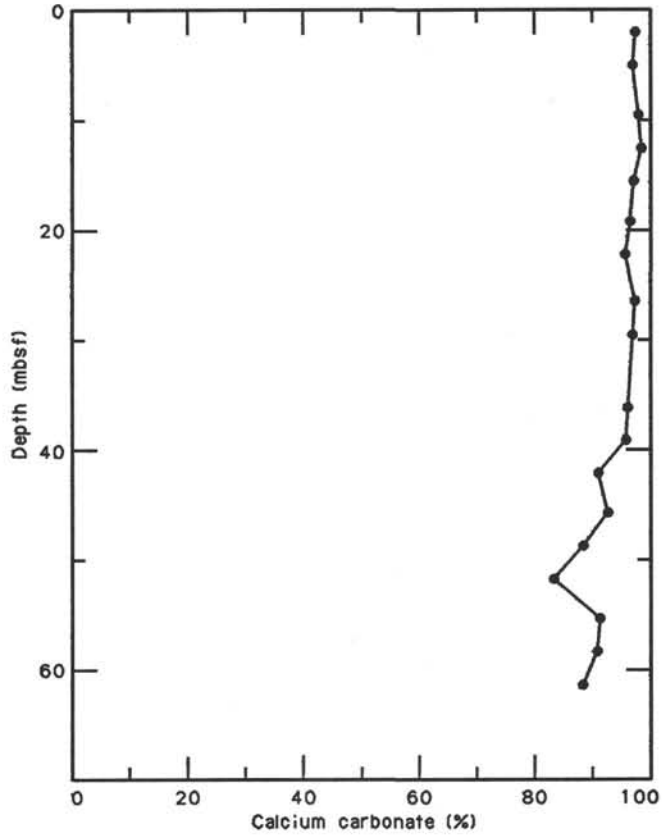

Figure 12. Calcium carbonate profile, Site 753.

Formation factor values, which range from 1.55 to 2.94, decrease slightly with increasing water content at 36 mbsf and increase at 52 mbsf in comparatively harder sediments (Table 8 and Fig. 13). This latter increase coincides with the increase in shear strength.

Thermal Conductivity

Thermal conductivities are shown in Table 9 and Figure 13. They range between 1.2 and 1.4 W/m°C. *In-situ* temperature measurements obtained at 24.20 and 53.43 mbsf are discussed

Table 7. Index properties and vane shear strength of sediments from Hole 753A.

Core, section, interval (cm)	Depth (mbsf)	Water content (%)	Porosity (%)	Density			Undrained shear strength (kPa)
				Wet bulk (g/cm^3)	Dry bulk (g/cm^3)	Grain (g/cm^3)	
1H-2, 80	2.30	41.52	65.53	1.64	0.96	2.71	6.1
1H-4, 80	5.30	39.25	63.44	1.66	1.01	2.72	3.5
2H-2, 80	9.80	41.23	64.94	1.62	0.95	2.67	3.2
2H-4, 80	12.80	40.45	64.33	1.65	0.98	2.69	5.5
2H-6, 80	15.80	44.63	68.32	1.58	0.88	2.70	0.7
3H-2, 80	19.50	39.07	62.83	1.65	1.00	2.67	1.4
3H-4, 80	22.50	38.10	59.71	1.67	1.03	2.44	5.1
4H-2, 80	26.70	36.40	60.56	1.71	1.09	2.72	3.0
4H-4, 80	29.70	37.50	62.22	1.70	1.06	2.78	2.9
5H-2, 80	36.30	49.57	72.48	1.52	0.77	2.71	9.9
5H-4, 80	39.30	46.23	69.33	1.55	0.83	2.66	9.1
5H-6, 80	42.30	43.16	66.53	1.59	0.90	2.65	12.6
6H-2, 82	45.92	37.57	61.36	1.70	1.06	2.67	
6H-4, 82	48.92	36.92	61.28	1.72	1.09	2.74	86.1
6H-6, 80	51.90	36.93	61.03	1.73	1.09	2.71	109.4
7H-2, 80	55.50	37.52	61.18	1.68	1.05	2.66	73.3
7H-4, 80	58.50	34.58	58.45	1.73	1.13	2.70	58.9
7H-6, 80	61.50	37.19	61.15	1.68	1.06	2.69	57.0

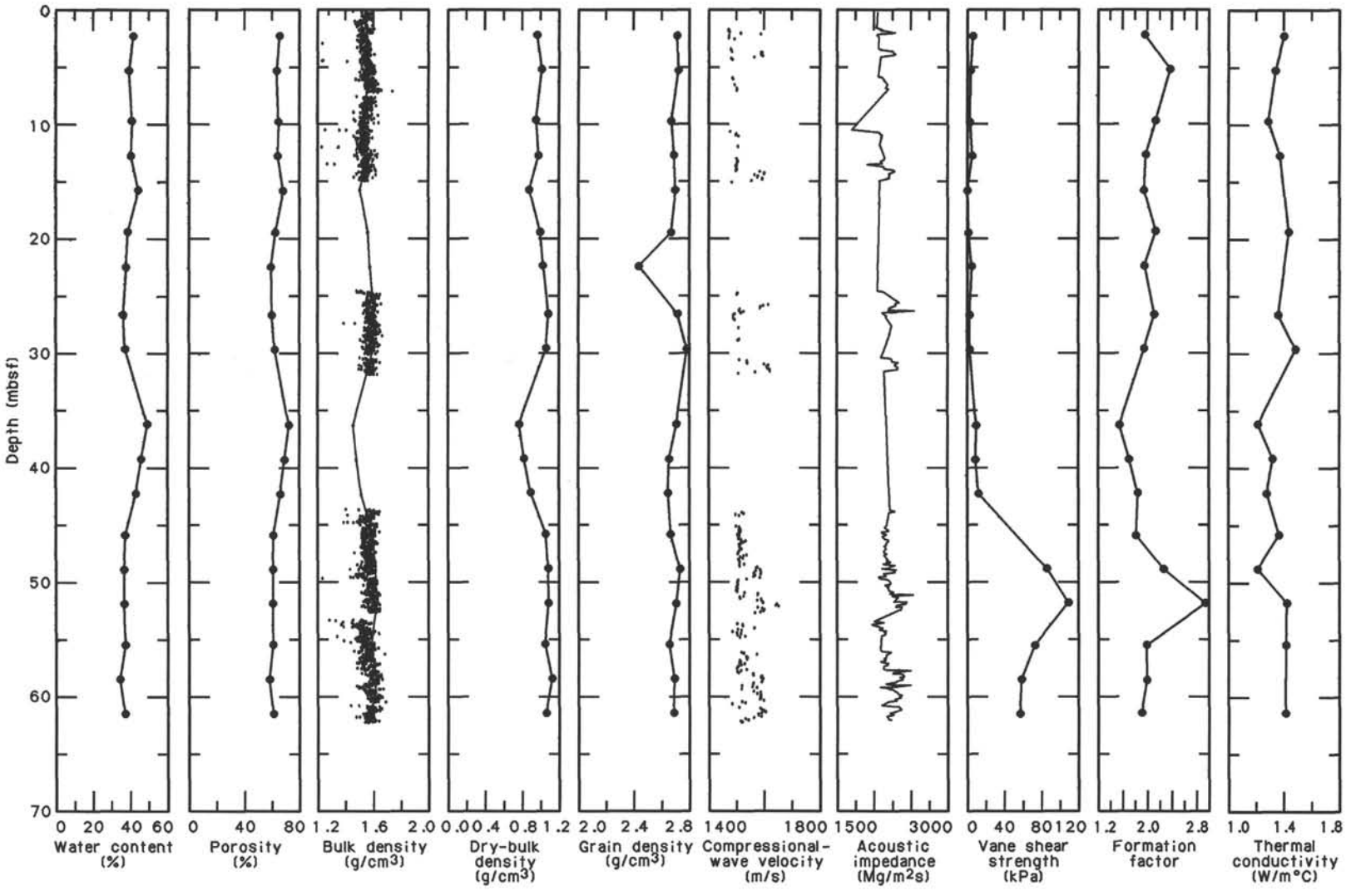

Figure 13. Index properties, compressional-wave velocity, acoustic impedance, vane shear strength, formation factor, and thermal conductivity profiles of sediments from Hole 753A.

Table 8. Formation factor of sediments from Hole 753A.

Core, section, interval (cm)	Depth (mbsf)	Formation factor
1H-2, 80	2.30	1.96
1H-4, 80	5.30	2.37
2H-2, 80	9.80	2.14
2H-4, 80	12.80	1.98
2H-6, 80	15.80	1.95
3H-2, 80	19.50	2.14
3H-4, 80	22.50	1.96
4H-2, 80	26.70	2.12
4H-4, 80	29.70	1.95
5H-2, 80	36.30	1.55
5H-4, 80	39.30	1.71
5H-6, 80	42.30	1.85
6H-2, 82	45.92	1.82
6H-4, 82	48.92	2.27
6H-6, 80	51.90	2.94
7H-2, 80	55.50	1.99
7H-4, 83	58.53	2.00
7H-6, 83	61.53	1.91

Table 9. Thermal conductivity of sediments from Hole 753A.

Core, section, interval (cm)	Depth (mbsf)	Thermal conductivity (W/m°C)
1H-2, 70	2.20	1.402
1H-4, 70	5.20	1.341
2H-2, 70	9.70	1.289
2H-4, 70	12.70	1.372
3H-2, 70	19.40	1.440
4H-2, 70	26.60	1.365
4H-4, 70	29.60	1.487
5H-2, 70	36.20	1.217
5H-4, 70	39.20	1.324
5H-6, 70	42.20	1.279
6H-2, 70	45.80	1.369
6H-4, 70	48.80	1.214
6H-6, 70	51.80	1.426
7H-2, 70	55.40	1.418
7H-6, 70	61.40	1.414

with the Site 752 results (see "Physical Properties" section, "Site 752" chapter).

Discussion

The nannofossil/foraminifer oozes cored at Site 753 display atypical physical properties relative to other oceanic calcareous oozes (Hamilton, 1976), with very low water content and nearly constant index properties with depth. Although the low water content and the low porosity are not conclusive evidence of winnowing or a lag depositional system, they do suggest removal of overburden. It is worth noting that the Neogene stratigraphic section at Site 753 is highly condensed in comparison to the same age section in Site 754 (see "Biostratigraphy" sections, this chapter and "Site 754" chapter, this volume). Despite the condensed section, the biostratigraphic results indicate a nearly complete section, with perhaps two hiatuses in the Miocene section. Historically, this section may have been exposed to short intervals of erosion, and/or nondeposition, resulting in the relatively constant, but overcompacted, aspect of these sediments. A minor change in the physical properties marks a sedimentary transition below 45 mbsf, where ooze changes into laminated chalk. This change is best observed in the measurements of vane shear and resistivity (formation factor).

SEISMIC STRATIGRAPHY

Site 753

Site 753 is on the northern margin of Broken Ridge, approximately 25 km north of the prominent southern scarp (Fig. 2). Site 753 was positioned to sample the youngest lithology below the prominent angular unconformity in order to further constrain the time interval over which the erosional event occurred. The youngest unit underlying the angular unconformity occurs along the northern edge of the ridge, immediately upslope from the subtle increase in seafloor gradient (Fig. 14). The nearly transparent acoustic character of this unit arises from the lack of any strong acoustic impedance contrasts, suggesting a uniform composition. The acoustically transparent unit is one of three seismic stratigraphic units that comprise the prograding downlapping sequence below the unconformity (Fig. 14). RC2708 seismic line 20 shows the thinning of the prograding downlapping sequence toward the north (Fig. 14).

Correlation Between Seismic Stratigraphy and Lithostratigraphy

Although continuous downhole sonic and density measurements (i.e., logging) were not conducted at Site 753, discrete compressional-wave and density measurements on samples from Cores 121-753A-1H to 121-753A-7H (0–62.8 mbsf) were used to calculate velocity and bulk-density data (Fig. 13, "Physical Properties" section, this chapter). The calculated velocities are in good agreement with those velocities derived from sonobuoy solutions for the pelagic cap, lithologic Unit I (Fig. 15). However, the downcore laboratory compressional-wave measurements for Unit II are lower than those derived from sonobuoys (Figs. 13 and 15). This discrepancy may arise from cracks and gaps caused by drilling disturbances in the section which would effectively diminish the compressional-wave propagation velocity through the medium. Thus, the sonobuoy velocity results for Unit II appear to be more reliable than the laboratory compressional-wave measurements. Sonobuoy velocity solutions and laboratory compressional-wave measurements downcore indicate average velocities of 1600 m/s for Unit I, and sonobuoy velocity solutions indicate an average velocity of 1800 m/s for Unit II (Figs. 13 and 15).

Acoustic impedance is the product of velocity and bulk density. Seismic reflectors arise from changes in acoustic impedance with depth. Accordingly, downcore acoustic impedance calculations in conjunction with seismic velocity allow correlation of the sampled lithostratigraphy at Site 753 and the seismic stratigraphy. Two major changes in acoustic impedance are noted at 14 and 24 mbsf (Fig. 13).

Pelagic Cap

The horizontal pelagic cap, lithologic Unit I, rests unconformably on the dipping and truncated limestone, chert, and chalk sequence (Fig. 14). Unit I onlaps the truncated and northward-dipping units and probably was deposited under the influence of both currents and relative sea-level changes. The depocenter for Unit I is 10 km south of Site 753 and was sampled at Site 754. The following reflectors are observed within the horizontal cap:

1. A faint reflector is observed both in the high-resolution seismic record and the 3.5-kHz precision depth recorder (PDR) record at 0.019 s TWT bsf (Figs. 16 and 17). The reflector coincides with a maximum in the mean grain size of the upper Miocene bulk sediment and corresponds to an increase in the acoustic impedance contrast at 14 mbsf. The coarser grain size may indicate a winnowed layer.

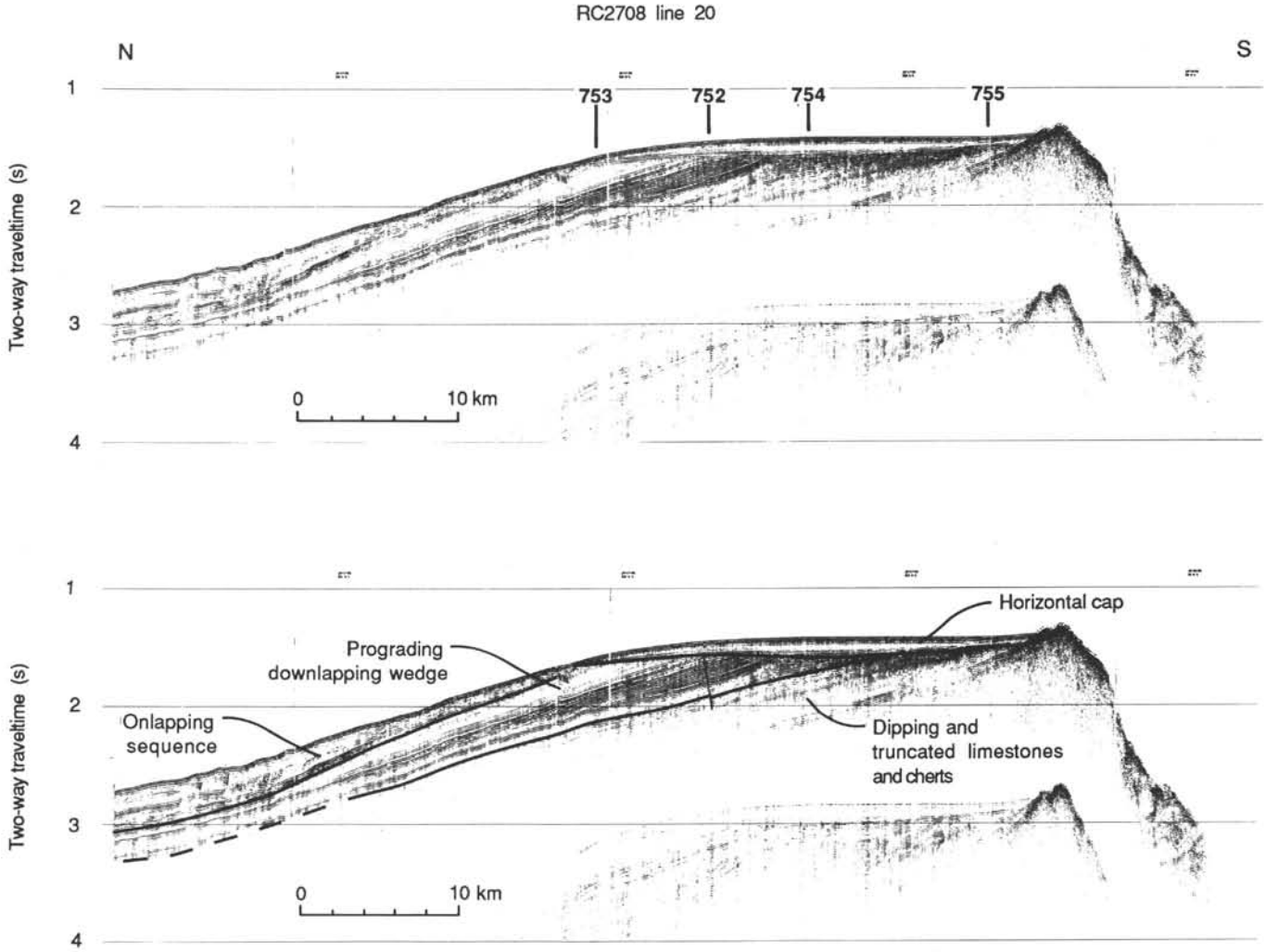

Figure 14. RC2708 single-channel seismic dip line 20 across Broken Ridge illustrating the stratigraphy observed on and surrounding the ridge. Site 753 penetrated the horizontal pelagic cap and bottomed in the acoustically transparent prograding sequence.

2. The second reflector, at 0.030 s TWT bsf in the high-resolution seismic record (Fig. 16), coincides with a hiatus separating upper Miocene foraminifer/nannofossil ooze (CN8) from underlying middle Miocene foraminifer/nannofossil ooze (CN4–5). A slight increase in the acoustic impedance contrast (24 mbsf) corresponds to this hiatus (Fig. 13). The cause of the acoustic impedance contrast is not clear, as there is no apparent change in lithology or grain size at 24 mbsf. However, the nannofossil ooze is noticeably stiffer in the bottom 10 m of Unit I relative to the overlying ooze. This increase in compaction could possibly engender the observed impedance contrast (Fig. 13).

3. An earlier erosional hiatus separating limestone pebbles in lower Miocene oozes (CN1,2; ~17–23.5 Ma) from underlying middle Eocene nannofossil chalk with foraminifers (CP13b; 47–49 Ma) is at 52 s TWT bsf (42 mbsf) in both the high-resolution seismic profile and the 3.5-kHz PDR record (Figs. 16 and 17).

Although Hole 753A was terminated at 62.8 mbsf (0.078 s TWT bsf) because the APC barrel could not be retrieved, the clearly truncated northward-dipping reflector is apparent on the 3.5-kHz PDR recording at 0.110 s TWT bsf (82 mbsf) (Figs. 16 and 17).

REFERENCES

Banner, F. T., and Blow, W. H., 1965. Progress in the planktonic foraminiferal biostratigraphy of the Neogene. *Nature*, 208:1164–1166.

Bé, A.W.H., and Tolderlund, D. S., 1971. Distribution and ecology of living planktonic foraminifera in surface waters of the Atlantic and Indian oceans. *In* Funnell, B. M., and Riedel, W. R. (Eds.), *Micropaleontology of Oceans*: Cambridge (Cambridge Univ. Press), 105–149.

Berggren, W. A., Kent, D. V., Flynn, J. J., and Van Couvering, J. A., 1985. Cenozoic geochronology. *Geol. Soc. Am. Bull.*, 96:1407–1418.

Blow, W. H., 1969. Late middle Eocene to Recent planktonic biostratigraphy. *In* Bronnimann, P., and Renz, H. H. (Eds.), *Proc. Int. Conf. Planktonic Microfossils, 1st, Geneva, 1967*, 1:199–421.

Bolli, H. M., Saunders, J. B., and Perch-Nielsen, K. (Eds.), 1985. *Plankton Stratigraphy*: Cambridge (Cambridge Univ. Press).

Fenner, J., 1984. Eocene-Oligocene planktic diatom stratigraphy in the low latitudes and in the high southern latitudes. *Micropaleontology*, 30:319–342.

Hamilton, E. L., 1976. Variations of density and porosity with depths in deep-sea sediments. *J. Sediment. Petrol.*, 46:280–300.

Jenkins, D. G., 1960. Planktonic foraminifera from the Lakes Entrance oil shaft, Victoria, Australia. *Micropaleontology*, 6:345–371.

_____, 1967. Planktonic foraminiferal zones and new taxa from the lower Miocene to the Pleistocene of New Zealand. *N. Z. J. Geol. Geophys.*, 10:1064–1078.

_____, 1971. New Zealand Cenozoic planktonic foraminifera. *N. Z. Geol. Surv. Paleontol. Bull.*, 42:1–278.

_____, 1978. Neogene planktonic foraminifers from DSDP Leg 40 Sites 360 and 362 in the southeastern Atlantic. *In* Bolli, H. M., Ryan, W.B.F., et al., *Init. Repts. DSDP*, 40: Washington (U.S. Govt. Printing Office), 723–739.

_____, 1985. Southern mid-latitude Paleocene to Holocene planktic foraminifera. *In* Bolli, H. M., Saunders, J. B., and Perch-Nielsen, K. (Eds.), *Plankton Stratigraphy*: Cambridge (Cambridge Univ. Press), 263–283.

Kennett, J. P., 1973. Middle and late Cenozoic planktonic biostratigraphy of the southwest Pacific DSDP Leg 21. *In* Burns, R. E., Andrews, J. E., et al., *Init. Repts. DSDP*, 21: Washington (U.S. Govt. Printing Office), 575–640.

Okada, H., and Bukry, D., 1980. Supplementary modification and introduction of code numbers to the low-latitude coccolith biostratigraphic zonation (Bukry, 1973; 1975). *Mar. Micropaleontol.*, 5:321–325.

Perch-Nielsen, K., 1985. Cenozoic calcareous nannofossils. *In* Bolli, H. M., Saunders, J. B., and Perch-Nielsen, K. (Eds.), *Plankton Stratigraphy*: Cambridge (Cambridge Univ. Press), 427–554.

Srinivasan, M. S., and Kennett, J. P., 1981. Neogene planktonic foraminiferal biostratigraphy: equatorial to subantarctic, South Pacific. *Mar. Micropaleontol.*, 6:499–534.

Toumarkine, M., and Luterbacher, H., 1985. Paleocene and Eocene planktic foraminifera. *In* Bolli, H. M., Saunders, J. B., Perch-Nielsen, K. (Eds.), *Plankton Stratigraphy*: Cambridge (Cambridge Univ. Press), 87–154.

Ms 121A-107

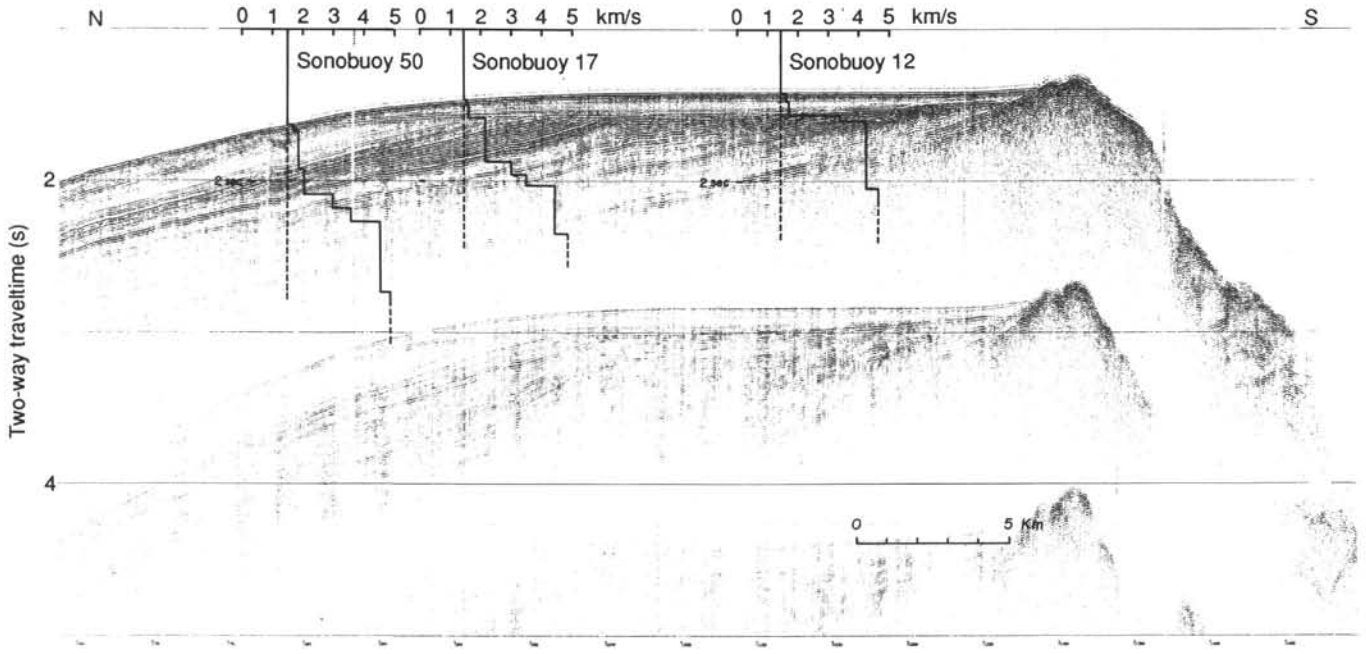

Figure 15. Sonobuoy velocity solutions from intersecting strike lines projected onto the dip line, correcting for changes in water depth. The downsection velocity gradient is also manifested downslope in response to the subcropping reflectors. There is good agreement between sonobuoy-derived velocities and laboratory-derived sonic velocities at Site 753.

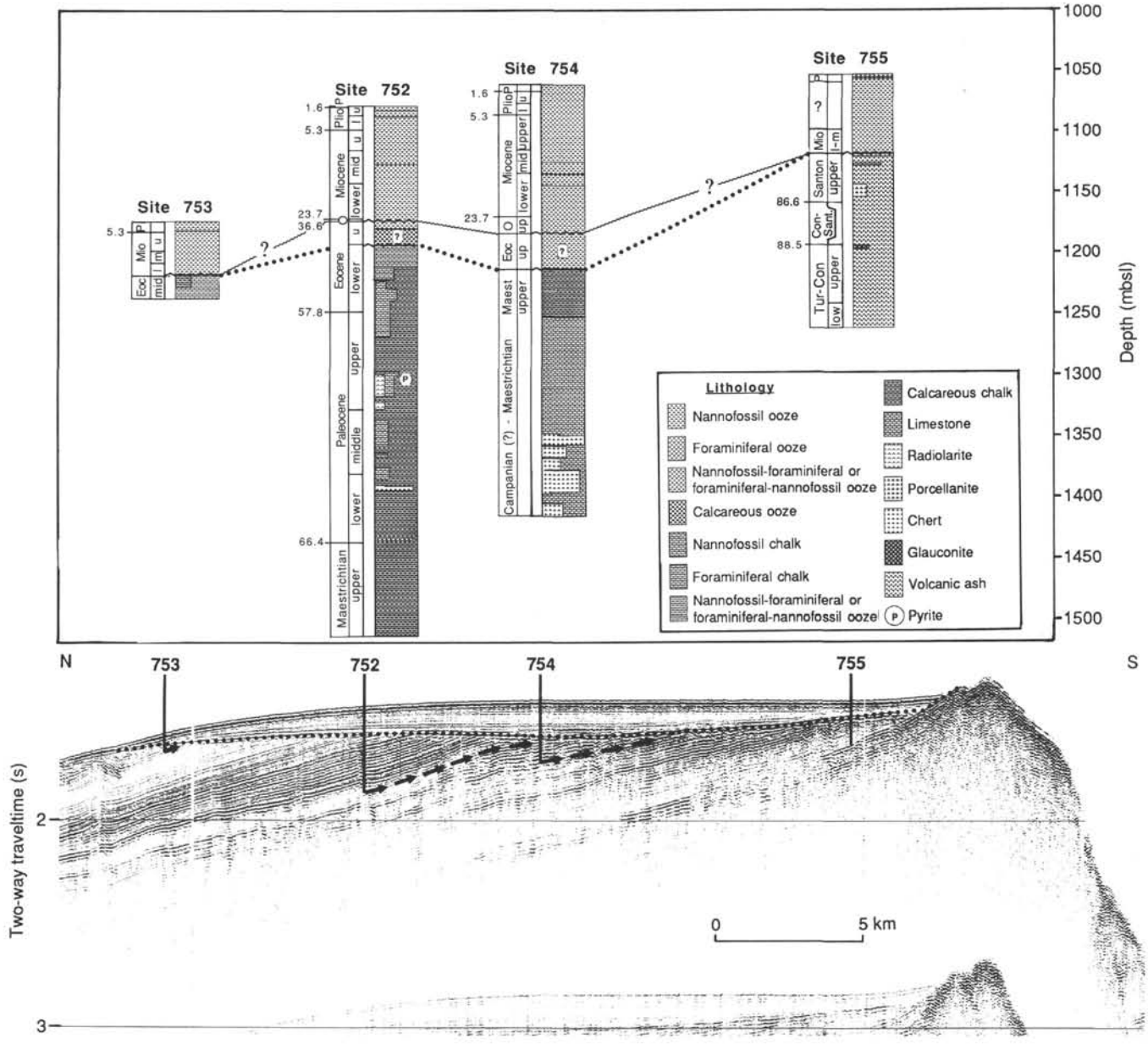

Figure 16. Correlation of seismic stratigraphy and lithostratigraphy sampled at Sites 752, 753, 754, and 755 on Broken Ridge. The arrows represent the upward continuation of the deepest horizon penetrated by Sites 752, 753, and 754 to the angular unconformity, illustrating the amount of stratigraphic section recovered and the stratigraphic overlap—if any—among the sites. The dotted line represents the middle Eocene hiatus and the wavy line denotes the Oligocene hiatus. The two hiatuses coalesce at Sites 753 and 755, but the question marks indicate that the position where they coalesce across Broken Ridge is not resolved.

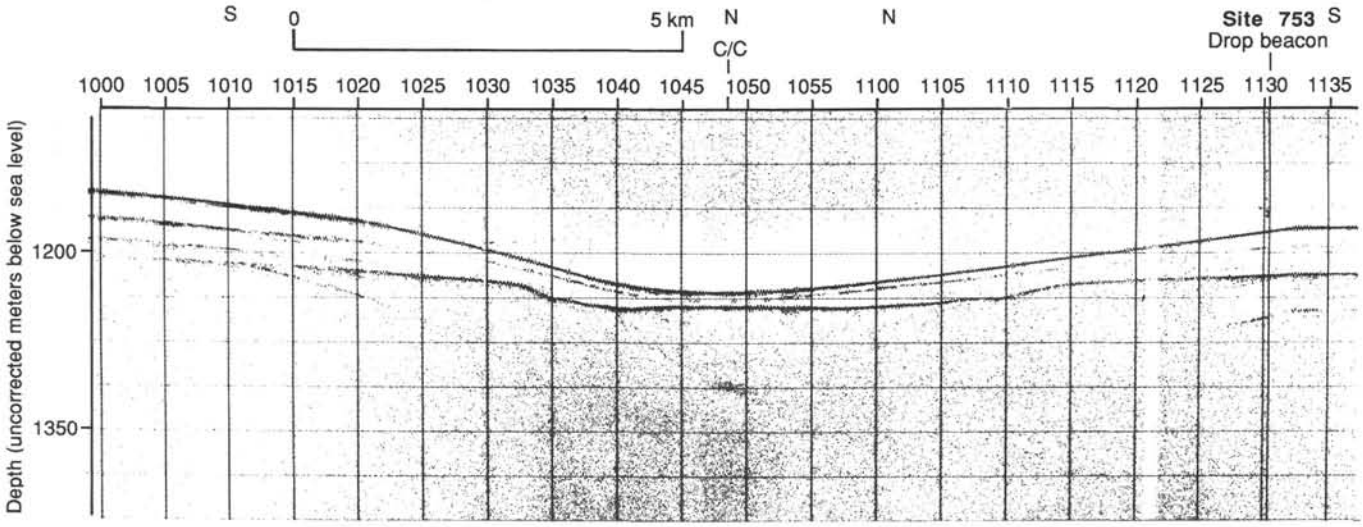

Figure 17. The 3.5-kHz PDR record over Site 753. The maximum acoustic penetration is approximately 100 m because of attenuation of the high-frequency signal. The 3.5-kHz profile augments the high-resolution seismic-reflection profile by providing a sonic character for shallow events that are at or below the vertical resolution of the water gun seismic system.